Approximate analytical solution of a (*V*,m,h) reduced system for backpropagating action potentials in sparsely excitable dendrites

Nicolangelo Iannella[1*], Roman R. Poznanski[2]

[1]The Faculty of Mathematics and Natural Sciences, University of Oslo, Oslo 0316 Norway

[2] Integrative Neuroscience Initiative, Melbourne, Australia 3145

*Correspondence: n.l.iannella@ibv.uio.no

Abstract

We derive an approximate analytical solution of a nonlinear cable equation describing the backpropagation of action potentials in sparsely excitable dendrites with clusters of transiently activating, TTX-sensitive Na$^+$ channels of low density, discretely distributed as point sources of transmembrane current along a continuous (non-segmented) passive cable structure. Each cluster or hotspot, corresponding to a mesoscopic level description of Na$^+$ ion channels, included known cumulative inactivation kinetics observed at the microscopic level. In such a reduced third-order system, the 'recovery' variable is an electrogenic sodium-pump and/or a Na$^+$- Ca^{2+} exchanger imbedded in the passive membrane, and a high leakage conductance stabilizes the system. A nonlinear cable equation was used to investigate back-propagation and repetitive activity of action potentials, exhibiting characteristics of the modified Hodgkin-Huxley kinetics (in the presence of suprathreshold input). In particular, a time-dependent analytical solution was obtained through a perturbation expansion of the membrane potential (*V*) for all voltage-dependent terms including the voltage-dependent Na$^+$ activation (m) and state-dependent inactivation (h) gating variables and then solving the resulting system of integral equations. It was shown that backpropagating action potentials attenuate in amplitude are dependent on the discrete and low-density distributions of transient Na$^+$ channels along the cable structure. A major significance of integrative modeling is the provision of a continuous description of the non-dimensional membrane potential (Φ) as a function of position.

Keywords: Sodium ions, spike trains, backpropagating action potentials, sparsely excitable dendrites, integrative modeling, ionic cable equation, Green's functions.

1. Introduction

The *ad hoc* application of computational modeling to excitable dendrites (exhibiting a variety of exotic membrane currents) has underestimated the epistemological limitations of the Hodgkin-Huxley (H-H) equations. Single-cell patch-clamping techniques have revealed a rich repertoire and diversity of voltage-dependent ion channels in the dendrites of almost all neurons. As well, dendrites contain an abundant number of ligand-gated channels and extrasynaptic receptors juxtaposed with voltage-dependent ion channels a discrete spatial location.

Action potential trains have been shown to backpropagate into the dendritic trees of several different varieties of neurons from electrophysiological recordings made with patch pipettes along its arbors e.g., (Golding et al., 2001; Stuart et al., 1997). Voltage-gated sodium (Na$^+$) channels on the somatodendritic surface of neurons have been mapped with patch-clamp recordings (e.g., Magee & Johnston, 1995; Stuart & Häusser,1994). However, insofar as the spatial distribution of individual sodium (Na$^+$) channels is concerned, the problem remains unresolved. In most circumstances, it is indirectly referred to and/or assumed to be non-sparse, uniform, or homogeneous. However, a homogeneous distribution does not imply a continuous distribution since recordings using patch-pipettes are measured discretely at a few selected points (Magee & Johnston 1995; Stuart & Häusser, 1994). The channel pores through which the Na$^+$ ions must flow to bring about an action potential are presumably only 10 Angstroms (or 0.001μm) in diameter. Therefore, a continuous distribution of channels is very difficult to show with patch-clamp analysis because a differential current density does not always imply distinct densities of channels, requiring an indefinite large number of patch-clamp estimates of channel density (for reviews, see Johnston et al.,1996; Migliore & Shepherd, 2002; Stuart & Spruston, 1995).

J. Multiscale Neurosci. Vol.2(2), 350-371

(©2023 The Authors) Published by Neural Press   350

Journal of Multiscale Neuroscience

Earlier studies with patch-pipettes revealed Na$^+$ channels to occur predominantly on the somata and along the primary dendrites of neocortical pyramidal cells (Huguenard et al., 1989; Stuart & Häusser, 1994). The predisposition for such localization was partly due to synapses impinging distally (and therefore leaving a greater accumulation of Na$^+$ channels for theproximal dendrites), which can invoke full-blown Na$^+$ action potentials initiated through strong synaptic stimulation (Regehr et al., 1993). Indeed, dendritic hotspots of glutamate sensitivity in neocortical pyramidal dendrites attest to the density distribution of synapses in distal regions of dendrites being sparsely distributed (Frick et al., 2001). However, there are exceptions, for instance, in some sensory neurons, like mitral cells of the olfactory bulb (Bischofberger & Jonas, 1997) and amacrine cells of the retina (Yamada et al.,2002) which appear to initiate dendritic action potentials with forward propagation to the soma in both mitral cells (Chen et al., 2002), and amacrines (Miller & Dacheux, 1976). Stuart & Häusser (1994) hypothesized that dendrites of Purkinje cells have a higher-threshold for action potential activation in comparison with the soma/axon hillock suggesting a low density of Na$^+$ channels and, therefore, resolving the issue of how dendritic Na$^+$ channels boost backpropagating action potentials (BAPs), while failing to support dendritic initiation. Indeed, dendritic spikes have a much slower time course of rise compared to action potentials which would indicate a relative sparseness of Na$^+$ channels, attributable to a high threshold for opening Na$^+$ gates, about 30mV.

In hindsight, a decreased membrane area exposed to voltage-dependent ionic channels (like Na$^+$ channels) as a consequence of impinging synaptic and extrasynaptic receptors (absent in axonal membrane), and the presence of Na$^+$ channels needed to elucidate both forward and BAPs, implies a uniform yet the sparse distribution of Na$^+$ channels in dendrites. In the case of the squid axon, the known density of Na$^+$ channels reaches 1000 μm^2 (Hodgkin, 1975), and the average distance between such channels is approximately 0.01 μm. Therefore, ion flows during nerve activity appear at sparsely distributed sites (Ehrenstein & Lecar, 1972). However, the effect of the discreteness on both the voltage and the kinetics of the membrane response may be negligible (Mozrzymas & Bartoszkiewicz, 1993). In the case of CA1 hippocampal dendrites, for example, the average density of Na$^+$ channels is only about 10 μm^2 (Magee & Johnston, 1995), leaving the average distance between such channels to be approximately

1 μm apart. Therefore, the effect of the discreteness between such channels will be apparent.

To develop realistic input/output functions of dendritic integration that incorporate all the complexities introduced by active dendrites in a biophysical model (Reyes, 2001), it is important to introduce a heterogeneous membrane with voltage-dependent ionic channels and, in particular, Na$^+$ channels as discrete macromolecules, sparsely distributed along dendrites (Hille, 2001). The modeling of such dendrites requires the enforcement of a heterogeneous excitable membrane rather than a 'weakly' or homogeneous excitable membrane, for which the former ascribes to a low density and a discrete spatial distribution of channels along the dendrites. In contrast, the latter does not ascribe to the discrete distribution of channels. Indeed, in earlier models of active dendrites, a low or diminished excitability (i.e., a low density of channels) through scaling the conductances without invoking a discrete spatial distribution of channels (see, e.g., Horikawa, 1998; Rapp et al., 1996; Sabah & Leibovic, 1972) was assumed. Evidence for a relatively sparse density in the spatial distribution of transient Na$^+$ channels comes indirectly from the observed decrement in the amplitude of BAPs trains affected by cable properties, including the distribution and locus of Na$^+$ channels and their prolonged inactivation (Jung et al., 1997), and slow inactivation (Callaway & Ross, 1995; Colbert et al., 1997; Jung et al., 1997; Mickus et al., 1999) as well as frequency-dependent dendritic Na$^+$ spike broadening (Lemon & Turner, 2000).

Williams & Stuart (2000) have identified two important factors controlling the modification of BAPs trains: (i) the recruitment of distal dendritic Na$^+$ and Ca^{2+} channels and (ii) the cumulative inactivation of dendritic Na$^+$ channels. To our knowledge, such mechanisms have not been incorporated into biophysically realistic models. This represents a significant challenge because earlier analytical work dealing with (V,m,h) reduced systems (see FitzHugh, 1960) failed to qualitatively reproduce the pulse recovery necessary for repeated firing for BAP trains. In an attempt at modeling such phenomena under current-clamp conditions, the so-called ionic cable theory, as advanced by Poznanski & Bell (2000a,b) (for small voltage perturbations from rest), can be extended to analytically solve such nonlinear problems for trains of BAPs along a dendritic arbor, with a spatially discrete distribution of Na$^+$ channels. This approach differs from previous approaches in that complete analytical resolution is

feasible without too many simplifying assumptions concerning the kinetics of gating currents. The Na$^+$ activation is not simply a function of voltage but also a function of time. Hence, reduced models which assume Na$^+$ activation to be sufficiently fast to be described by its equilibrium value are too simplistic and inappropriate for modeling BAPs *in vivo* (e.g., Casten et al., 1975; Kepler et al., 1992; Krinskii & Kokoz, 1973; Penney & Britton, 2002; Rinzel,1985; Wilson, 1999).

The need for a new cable-modeling methodology is twofold. Firstly, compartmental models used to study BAPs (see, e.g., Antic, 2003; Doiron et al., 2001; Lüscher & Larkum, 1998; Mainen et al., 1995; Migliore, 1996; Rapp et al.,1996), discretize the continuous membrane of the neuron into a discrete set of interconnected isopotential compartments that leads to presumptive conclusions such as 'local- subunits' in dendrites (Mel 1993; Poirazi et al., 2003). However, the spatially discretized nature of voltage and channel kinetics employed in compartmental models warrants a closer look. During initial voltage that results from a localized action potential, large amplitude voltage gradients leave the membrane potential in an isopotential state. Secondly, numerical methods like compartmental models suffer from too many degrees of freedom resulting in a non-uniqueness problem. This has been succinctly articulated by Frankenhaeuser & Huxley (1964), p.306: "*The equation system is so involved that it is impossible in most cases to get even a fair idea of the effect of a change of a single value without going through a complete computation.*" In other words, the non-uniqueness problem and the accumulation of numerical errors can raise concerns about the uniqueness and accuracy, typically requiring that each time a single parameter change occurs, a complete evaluation of the entire set of equations is required.

The main issue of our concern is the conclusions made by Van Ooyen et al. (2002) and Schaefer et al. (2003) that subtle structural differences in morphology within a population of neurons are sufficient to explain the functional variability in dendritic function. This is in agreement with earlier studies showing that branch points (equivalent to a step decrease in the cable diameter) could behave as a point of higher excitability referred to as a 'hotspot' (Dimitrova & Dimitrov 1991), but contrasts with the conceptual presumption that the

spatial distribution of identical ion channels in a particular class of neurons has significant functional importance in determining intraneuronal infor-mation processing (Holden, 1981). Thus, the notion of BAPs depending primarily on morphology (i.e., electrotonic geometry) rather than membrane properties can be tested using ionic cable theory by showing that the spatial localization of distributed ion channels in non-space-clamped structures does matter functionally. Geometrical inhomogeneities (i.e.,step decrease in the cable diameter or a branch point) *per se* are morphological but, to a lesser extent, functional formations (see Altenberger et al., 2001).
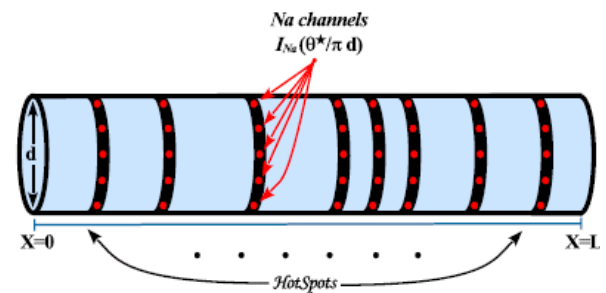

Figure 1: *A schematic illustration of a dendrite of diameter d (μm) studded with clusters or hotspots of Na$^+$ ionic channels. The arrow above the hotspot reflects the notion of I_{Na} representing a point source of transmembrane current imposed on an infinitesimal area on the cable. The symbol N denotes the number of hotspots, and N*' denotes the number of Na$^+$ channels in each hotspot per membrane surface of the cable, represented schematically as dark spots. The total number of Na$^+$ channels is given as NN*'.*

The notion behind ionic cable theory is to incorporate the density distribution of specific proteins subdivided into two classes, carriers and pores (ion channels), into passive cable models of neural processes by distributing these specific voltage-dependent ionic currents discretely. In particular, we will consider an all Na$^+$ system like that found in rabbit myelinated axons (Chiu et al., 1979) or pyramidal dendrites in the electrosensory lateral-line lobe of weakly electric fish (Turner et al. 1994) with discrete loci of Na$^+$ channels or hotspots as active point sources of transmembrane current, imposed on a homogeneous (non-segmented) leaky cable structure with each hotspot assumed to occupy an infinitesimal region containing a small cluster of fast pores called Na$^+$ channels in the presence of ion fluxes due to active transport processes, such as Na$^+$- Ca^{2+} exchanger and Na$^+$-pump imbedded in the lipid bilayer membrane as proteins specialized as slow carriers.

2. The cable equation for discretely imposed Na^+ channels

Let $V(x, t)$ be the depolarization along a cable (i.e., membrane potential less the resting potential) in mV, and let I_{Na} be the nonlinear functional of membrane potential representing the transmembrane Na^+ current density per unit membrane surface of dendritic cable in (mA/cm). The voltage response (or depolarization) along a leaky cable representation of a cylindrical passive dendritic segment with ionic channels occurring at discrete points along the cable (see **Fig.** 1) satisfies the following cable equation:

$$
\begin{aligned}
C_m \frac{\partial V}{\partial t} =\ & \frac{d}{4\rho_i}\frac{\partial^2 V}{\partial x^2} - \frac{V}{R_m} \\
& + \sum_{i=1}^{N} I_{Na}(x, t; V)\delta(x - x_i) \\
& + \sum_{j=1}^{N} I_{Na-Ca}\delta(x - x_j) \\
& + \sum_{z=1}^{N} I_{Na(pump)}\delta(x - x_z),
\end{aligned}
\tag{1}
$$

where x is the distance in cm, time t is in msec, d is the diameter of the cable in cm, $C_m = c_m/\pi d$ is the membrane capacitance per unit area (F/cm^2), $R_m = r_m\pi d$ is the membrane resistivity (Ωcm^2), $\rho_i = r_i\pi d^2/4$ is the cytoplasmic resistivity (Ωcm), N is the number of clusters of Na^+ channels or hotspots (dimensionless), I_{Na-Ca} is the sodium-calcium exchanger current density in mA/cm, $I_{Na(pump)}$ is the sodium-pump current density per unit membrane surface of dendritic cable in mA/cm, and δ is the Dirac-delta function reflecting the axial position along the cable where the ionic current is positioned in cm^{-1} (see FitzHugh,1973) with the suprathreshold (current) injection at location $x = 0$, the pump location at $x = x_z$, and ionic channel locations at $x = x_i$.

Equation (1) can be cast in terms of non-dimensional space and time variables, $X = x/\lambda$ and $T = t/\tau_m$, respectively, where $\lambda = (R_m d/4 \rho_i)^{1/2}$ and $\tau_m = R_m C_m$ are, respectively, the space and time constants in cm and msec. Thus Eqn (1), after using $\delta(\lambda X) = \delta(X)/\lambda$, becomes

$$
\begin{aligned}
\frac{\partial V}{\partial T} =\ & \frac{\partial^2 V}{\partial X^2} - V \\
& + \frac{R_m}{\lambda}\sum_{i=1}^{N} I_{Na}(X, T; V)\delta(X - X_i) \\
& + \frac{R_m}{\lambda}\sum_{j=1}^{N} I_{Na-Ca}\delta(X - X_j) \\
& + \frac{R_m}{\lambda}\sum_{z=1}^{N} I_{Na(pump)}\delta(X - X_z),
\end{aligned}
\tag{2}
$$

where $T > 0$, $0 < X < L$, l is the physical length in cm, $L = l/\lambda$ is the electrotonic length, $X = x/\lambda$ represents loci along the cable of ionic current, expressed in terms of the dendritic space constant λ, and I is the nonlinear transient Na^+ transmembrane current density per unit membrane surface of cable ($\mu A/cm$) (expressed as a sink of current since by convention inward current is negative and outward is positive) based upon the H-H gate formalism and the constant-field equation (Chiu et al., 1979; Dodge & Frankenhaeuser, 1959; Frankenhaeuser & Huxley, 1964):

$$
\begin{aligned}
I_{Na}(X, T; V) =\ & P_{Na}m^2(V)h(V)\lambda[Na^+]_e\left(\frac{V\mathcal{F}^2}{RT}\right) \\
& \times \left(\frac{(\exp[(V - V_{Na})\mathcal{F}/RT] - 1)}{(\exp(V\mathcal{F}/RT) - 1)}\right)
\end{aligned}
\tag{3}
$$

with $\mathcal{F}$, R, and T are the Faraday-constant ($\mathcal{F} = 96480$ C/mol), the gas constant ($R = 8.315$ $J/K/mol$), and the absolute temperature ($T = 273.15$ K), P_{Na} is the maximum permeability of Na^+ ions ($\mu m/sec$), $[Na^+]_e$ is the external Na^+ concentration in mM, $V_{Na} = E_{Na} - E_R$, $E_R = -70$ mV is the resting membrane potential, and $E_{Na} = 65$ mV is the Na^+ equilibrium potential conductance, which is similar but not equivalent to the permeability, i.e.,

$$
\mathcal{F}P_{Na}\lambda[Na^+]_e(\mathcal{F}/RT) \rightarrow g_{Na},
\tag{4}
$$

where g_{Na} denotes the maximum N^+ conductance per unit membrane surface of cable ($\mu S/cm$) given by (Hodgkin 1975):

$$
g_{Na} = g_{Na}^* N^*
\tag{5}
$$

and N^* is the number of transient Na^+ channels per unit membrane surface of cable in cm^{-1}, and $g_{Na}^* = 18pS$ is the maximum attainable conductance of a single Na^+ channel (Sigworth & Neher,1980; Stühmer et al., 1987). Possible nonuniform

distribution of channels can be determined from Eqn (5) by redefining the number of channels as a function of space, i.e., $g_{Na}(X) = g^*_{Na} N^*(X)$ so that at location $X = X_i$ there will be $N^*(X_i) = \theta(X_i)/\pi d$ Na^+ channels, where $\theta(X_i) \equiv \theta_i$ is the number of Na^+ channels per ith hotspot and assumed to be a nonuniform function with distance along the cable. For a nonhomogeneous distribution with greater occurrence on somata and near the primary branches of large dendrites, an appropriate function could be exponentially decaying in the somatofugal direction $\theta_i = \rho \exp(\gamma_{Na} X_i)$ where $\gamma_{Na} > 0$ and $\rho > 0$ are constants.

3. Scaling the macroscopic Na^+ current density

A mesoscopic Na^+ current density at discrete loci along the dendritic cable associated with only a low density of Na^+ channels can be approximated heuristically from a nonlinear (instantaneous) input I-V (i_{NaP}) relationship obtained by Hodgkin & Huxley (1952) based on observations of macroscopic currents at different voltages using the voltage-clamp technique. A space-clamp of the membrane and a voltage clamp of that membrane allowed them to set and hold the membrane potential at a particular value to determine the underlying ionic current. Such currents are macroscopic because they reflect an assemble average of many localized Na^+ channels. However, the effects of electromagnetic properties on dendritic structure produce an inadequate space-clamp upon signal properties, making it unlikely to predict a 'whole-cell' current from somatic recording. In practice, however, the value of I_{Na} along the cable at loci X_i will be determined from the value of V at that point. Therefore, an equation analogous to Cole's theorem could connect the membrane I-V relation (I_{Na}) with the input $I-V$ relation (i_{Na}) obtained using a single-channel patch-pipette recording. This is because, in most cases, the input $I-V$ relation is less nonlinear than the membrane $I-V$ relation as expressed by the relationship:

$$I_{Na} = \left(\frac{\rho_i}{\pi d^2}\right) \left\{ \frac{i_{Na}}{\left[\frac{dV_o}{di_{Na}} - \frac{dV_L}{di_{Na}}\right]} \right\}, \qquad (6)$$

where V_o and V_L represent (dimensional) V at $X = 0$ and $X = L$, respectively, in practice, Eqn (6) is limited to using a dual intracellular recording method to measure the voltage at two distinct points in the presence of pharmacological agents, which block all

other voltage-dependent ion channels that could intrude at those particular chosen loci. Theoretically, the H-H gating formalism can be replaced using Eqn (6) as a heuristic approximation of the macroscopic Na^+ current density. However, it is experimentally difficult to yield a dual-patch estimate at both ends of a dendrite (Schaefer et al., 2003).

The assumption that the "whole-cell" conductance equals the single channel conductance times the number of channels is limited to the somata of neurons as dendrites are rarely perfectly space-clamped, so determining the number of channels at the soma could, in principle, only approximate the number per unit surface of a dendrite. As it is experimentally difficult to obtain a true estimate of the "whole-cell" conductance, a spatial "scaling" of the macroscopic Na^+ current is performed through a spatial "scaling" parameter ϵ because, unlike the "whole-cell" macroscopic current, the current per dendritic patch involves only a small cluster of Na^+ channels. Hence, in the analysis that follows, ϵ will be considered small. Thus, the Na^+ transmembrane current density per unit membrane surface of cable ($\mu A/cm$) represented by Eqn (3) and expressed in terms of a conductance Eqn (7) and can be approximated as follows:

$$I_{Na}(X,T;V) \approx \epsilon g_{Na}\mu^2(V)\eta(V)V$$
$$\times \left(\frac{(\exp[(V - V_{Na})\mathcal{F}/RT)] - 1)}{(\exp(V\mathcal{F}/RT) - 1)}\right), \qquad (7)$$

where $\epsilon << 1$ is a small parameter calling the 'whole-cell' macroscopic transmembrane current density of Na^+ channels, and $\mu(V)$, $\eta(V)$ represent ensemble averages of the activation and inactivation gating variables, respectively, of the mesoscopic current density per unit length the mesoscopic current density per unit length of cable (dimensionless). It should be noted that the macroscopic current density is a good representation of reality for large θ_i ($>>100$), compared to the mesoscopic current density, which is a good representation for moderate values of θ_i ($>> 1$). For example, Hodgkin (1975) estimated an optimum density of Na^+ channels to be about $\theta_i = 500/\mu m^2$ in a $0.1\mu m$ diameter axon of the squid, while (Magee & Johnston, 1995) estimated the number of channels per patch to average at $\theta_i = 7/\mu m^2$ in the dendrites of rat hippocampal CA1 pyramidal neurons.

The constant-field model of ion permeation is based on steady-state, so the concentration is a function of distance only, and so is the presence of the space-constant (λ) in Eqn. (3) is because of the conversation from dimensional to non-dimensional space variable of ionic flux due to diffusion in accordance with Fick's principle. The macroscopic Na$^+$ current across the axon membrane of the giant squid was shown by (Hodgkin & Huxley, 1952) to follow a simple linear Ohmic relationship expressed through a driving term for the ionic current ($V - V_{Na}$) under the voltage-clamp conditions when the membrane potential is fixed and the instantaneous transmembrane current density per unit membrane surface of the cable is represented through a linear relationship (Hodgkin & Huxley, 1952):

$$I_{Na} = g_{Na} m^3(V) h(V) (V - V_{Na})$$

The state variables can be readily solved (Hodgkin & Huxley, 1952):

$$m[V(T)] = m_\infty + \{m[V(0)] - m_\infty\} \exp\left(-T\tau_m/\tau_\mu\right)$$
$$h[V(T)] = h_\infty + \{h[V(0)] - h_\infty\} \exp\left(-T\tau_m/\tau_h\right),$$

where $m_\infty = \alpha_m/(\alpha_m + \beta_m)$ and $h_\infty = \alpha_h/(\alpha_h + \beta_h)$ are the steady-state values of the activation $m[V(T)]$ and inactivation $h[V(T)]$, respectively, $\tau_\mu = 1/(\alpha_m + \beta_m)$ and $\tau_h = 1/(\alpha_h + \beta_h)$ are both time-constants, and the rate-constants ($msec$)$^{-1}$ are:

$$\alpha_m = 0.1(25 - V)/\{\exp[(25 - V)/10] - 1\}$$
$$\beta_m = 4\exp(-V/18)$$
$$\alpha_h = 0.07\exp(-V/20)$$
$$\beta_h = 1/\{\exp[(30 - V)/10] + 1\}$$

This approximation does not necessarily apply to other membranes, where for example, ionic flux across the dendrite's membrane is represented by the constant-field equation of electrodiffusion (cf. Pickard, 1974). If the electrodiffusion of Na$^+$ current across the dendritic membrane 'barrier' is assumed to be nonlinear, then the driving forces due to concentration gradients must be replaced with the constant-field equations, which take into account the effect of the ion concentrations in the membrane (Vandenberg & Bezanilla 1991). This is especially prevalent at hotspots when spatial ionic concentration changes are expected to be large (Qian & Sejnowski 1989). In addition to a barrier, there are 'membrane gates' controlling the flow of Na$^+$

(ionic) current, with the time-dependent gating having a lower power for activation from the standard H-H model (Chiu et al. 1979; Dodge & Frankenhaeuser, 1959; Frankenhaeuser & Huxley, 1964).

4. Analytical time-dependent solutions for active BAPs

A point near a fictitious soma is current-clamped to an action potential response. Here, we take $X = 0$ to be a point current-clamped to a functional representation of a single "somatic" nerve impulse (Chiang, 1978):

$$V(0, T) \equiv U(T) = U_o\left\{ \sin\left(\frac{2\pi}{5}\mathcal{A}T\right)e^{-0.2\mathcal{A}T} + 150e^{-2\mathcal{A}T} - 100e^{-4\mathcal{A}T} - 50e^{-1.2\mathcal{A}T}\right\}, \quad (8)$$

where U_o is the maximum potential (mV), and that can be further extended to include a train of BAPs:

$$\begin{aligned} V(0, T) &= \sum_{k=0}^{\mathcal{R}} U(T)H(T - k\omega) \\ &= \sum_{k=0}^{\mathcal{R}} U_o\left\{ \sin\left(\frac{2\pi}{5}\mathcal{A}(T - k\omega)\right)e^{-0.2\mathcal{A}(T-k\omega)} \right. \\ &\quad + 150e^{-2\mathcal{A}(T-k\omega)} - 100e^{-4\mathcal{A}(T-k\omega)} \\ &\quad \left. - 50e^{-1.2\mathcal{A}(T-k\omega)}\right\}H(T - k\omega), \end{aligned} \quad (9)$$

where k is an index, $\mathcal{A}$ is a scaling factor, R indicates the number of action potentials in the spike train, ω is the dimensionless interspike interval, and $H(.)$ is the Heaviside step function. Equation (9) yields the time course of the spike train at a single point, namely $X=0$. We focus on determining the time course of active backpropagation of action potentials in non-space-clamped cables as a perturbation from the "somatic" train of BAPs. This is accomplished by solving the following equation by inserting Eqn. (7) into Eqn. (2) and adding Eqn (9):

$$\begin{aligned} \frac{\partial V}{\partial T} &= \frac{\partial^2 V}{\partial X^2} - V \\ &+ \epsilon g_{Na}\frac{R_m}{\lambda}\sum_{i=1}^{N} \mu^2(V)\eta(V)V\left(\frac{e^{(V-V_{Na})\mathcal{F}/RT} - 1}{e^{V\mathcal{F}/RT} - 1}\right) \\ &\qquad\qquad \times \delta(X - X_i) \\ &+ \frac{R_m}{\lambda}\sum_{j=1}^{N} I_{Na-Ca}\delta(X - X_j) \\ &+ \frac{R_m}{\lambda}\sum_{z=1}^{N} I_{Na(pump)}\delta(X - X_z) \\ &+ \sum_{k=0}^{\mathcal{R}} U(T)H(T - k\omega)\delta(X). \end{aligned} \quad (10)$$

Although Eqn ([10]) is expressed in terms of non-dimensional space and time variables, the membrane potential must be non-dimensionalized by some characteristic value. A reasonable value would be the peak (amplitude) of the "somatic" spike U_{peak}. Hence, the non-dimensionalized membrane potential is expressed as:

$$\Phi \rightarrow V/U_{peak},$$

which allows us to rewrite Eqn. ([10]) as follows:

$$
\frac{\partial \Phi}{\partial T} = \frac{\partial^2 \Phi}{\partial X^2} - \Phi
$$

$$
+ \epsilon g_{Na} \frac{R_m}{\lambda} \sum_{i=1}^{N} \mu^2(\Phi)\eta(\Phi)\Phi \left(\frac{e^{(\Phi-\Phi_{Na})U_{peak}\Lambda} - 1}{e^{\Phi U_{peak}\Lambda} - 1} \right)
$$

$$
\times \delta(X - X_i)
$$

$$
+ \frac{R_m}{\lambda U_{peak}} \sum_{j=1}^{N} I_{Na-Ca}\delta(X - X_j) \qquad (11)
$$

$$
+ \sum_{k=0}^{\mathcal{R}} U(T)/U_{peak}H(T - k\omega)\delta(X),
$$

where $\Lambda = \mathcal{F}/RT$ (mV). Most studies that examine traveling wave solutions to nonlinear reaction-diffusion equations like Eqn ([11]) use a similarity transformation of the independent variables, such as $\xi \rightarrow X$–cT (see, e.g., Scott, 2002). However, a sparse density distribution of ionic channels along the dendrite results in the conduction velocity (c) being not constant (see Poznanski, 2001). Hence, leading-edge approximation of the H-H equations will not yield traveling wave solutions as previously explored (e.g., Rissman, 1977).

In the present theory, the maintenance of zero ionic currents at rest is accomplished with a sodium–pump, which counters the resting ionic fluxes to maintain equilibrium so that ionic conductances are at their resting values and the membrane potential returns to the resting state. The pumping rate appears to depend on the internal concentrations of Na^+, and the currents in the giant squid axon are always negligible (Moore & Adelman Jr., 1961). In small dendrites, however, with much smaller volume-to-surface ratios than for squid axon, for a 0.1 μm diameter at least 5000 times smaller (Hodgkin, 1975), the metabolic pump activity is sufficiently greater because only a few BAPs will affect the internal ionic composition. In such a case, the Na^+ pump could play a significant role in the ionic fluxes of the action potential. Consequently, the current balance equation at the site of the hotspot reads:

I_{Na}-P-$I_{Na-Ca} = 0$, where P is the outward Na^+ pump current density and

$$
I_{Na-Ca} = \kappa_{Na-Ca}\Big([Na^+]_i^3 [Ca^{2+}]_e^2
$$

$$
\times \exp\left[r(\Phi U_{peak} + E_R)\Lambda \right]
$$

$$
- \kappa_{Na-Ca} [Na^+]_e^3 [Ca^{2+}]_i^2
$$

$$
\times \exp\left[r(\Phi U_{peak} + E_R)\Lambda \right] \Big)
$$

where κ_{Na-Ca} is a scaling constant representing the density of exchanger molecule in the membrane ($pA/cm/mM$), $[Na^+]_i$ and $[Na^+]_e$ are concentrations of Na^+ in the intracellular and extracellular space (mM), respectively, $[Ca^{2+}]_i$ and $[Ca^{2+}]_e$ are concentrations of Ca^{2+} in the intracellular and extracellular space (mM), respectively, and r ($0 < r \leq 1$) is the position of an energy barrier in the plasma membrane defined by Eyring theory of reaction rates (dimensionless).

Suppose electroneutrality is maintained everywhere by virtue of equal concentrations, then $[Ca^{2+}]_e = [Ca^{2+}]_i$, and if all Ca^{2+} channels are assumed to be completely blocked, then $[Ca^{2+}]_e = 0$ and $[Ca^{2+}]_i = 0$, and therefore $I_{Na-Ca} = 0$. If the outward Na^+ pump current density is positive (by convention) and resting potential $\Phi_R = \Phi(0, 0) = 0$, then upon using L'Hopital's rule:

$$
I_{Na(pump)} = \frac{\epsilon g_{Na}\mu_o^2\eta_o \left(1 - \exp\left[-\Phi_{Na}U_{peak}\Lambda \right] \right)}{\Lambda} \qquad (12)
$$

where $\mu_o \equiv \mu(0)$ and $\eta_o \equiv \eta(0)$.

Assuming the hotspot location $X=X_i$ and the Na^+ pump location $X = X_z$ are juxtaposed and inserting $I_{Na-Ca}=0$ together with Eqn. ([12]) into Eqn ([11]) yields

$$
\frac{\partial \Phi}{\partial T} = \frac{\partial^2 \Phi}{\partial X^2} - \Phi
$$

$$
+ \epsilon g_{Na} \frac{R_m}{\lambda} \sum_{i=1}^{N} \left(\mu^2(\Phi)\eta(\Phi)\Phi \left[\frac{e^{(\Phi-\Phi_{Na})U_{peak}\Lambda} - 1}{e^{\Phi U_{peak}\Lambda} - 1} \right] \right.
$$

$$
\left. + \frac{\mu_o^2\eta_o}{\Lambda}\left[1 - e^{-\Phi_{Na}U_{peak}\Lambda} \right] \right)\delta(X - X_i)
$$

$$
+ \sum_{k=0}^{\mathcal{R}} U(T)/U_{peak}H(T - k\omega)\delta(X), \qquad (13)
$$

One can decompose the solution of Eqn (13) and represent it as a sum of two solutions of cable equations at some arbitrary point along the cable $X = X_p$:

$$\Phi_p(T) = \Phi_{op}(T) + \epsilon\Phi_{1p}(T)$$

where $\Phi_{op}(T)$ is the solution of a linear diffusion equation ($\epsilon = 0$):

$$\frac{\partial\Phi_o}{\partial T} = \frac{\partial^2\Phi_o}{\partial X^2} - \Phi_o + \sum_{k=0}^{\mathcal{R}}\frac{U(T)}{U_{\text{peak}}}H(T - k\omega)\delta(X) \tag{14}$$

and $\Phi_{1p}(T)$ remains the solution of a nonlinear reaction-diffusion system ($\epsilon \neq 0$):

$$\frac{\partial\Phi_1}{\partial T} = \frac{\partial^2\Phi_1}{\partial X^2} - \Phi_1 + \epsilon g_{\text{Na}}\frac{R_m}{\lambda}\sum_{i=1}^{N}$$
$$\times\left(\mu^2(\Phi_1)\eta(\Phi_1)\Phi_1\left[\frac{e^{(\Phi_1-\Phi_{\text{Na}})U_{\text{peak}}\Lambda} - 1}{e^{\Phi_1 U_{\text{peak}}\Lambda} - 1}\right]\right.$$
$$\left.+ \frac{\mu_o^2\eta_o}{\Lambda}\left[1 - e^{-\Phi_{\text{Na}}U_{\text{peak}}\Lambda}\right]\right)\delta(X - X_i) \tag{15}$$

As described in Iannella & Tanaka (2006) and Poznanski (2004), considering hotspots to act as point current sources permit Eqn (13) to be reformulated as a nonlinear Volterra integral equation through the application of the Green's function method of solution to Eqn (14)and Eqn (15) (see **Appendix**), Eqn. (13) can be expressed in terms of a Green's function G as follows,

$$\Phi_P(T) = \int_0^T\left[\sum_{k=0}^{\mathcal{R}}\left(\frac{U(s)}{U_{\text{peak}}}\right)H(s - k\omega)G_{po}(T - s)\right.$$
$$+ \epsilon\left(\frac{g_{\text{Na}}R_m}{\lambda}\right)\sum_{i=1}^{N}\left\{\mu^2[\Phi_i(s)]\eta[\Phi_i(s)]\Phi_i\right.$$
$$\left.\left.\times\left[\frac{e^{(\Phi_i-\Phi_{\text{Na}})U_{\text{peak}}\Lambda} - 1}{e^{\Phi_i U_{\text{peak}}\Lambda} - 1}\right]\right\}G_{pi}(T - s)\right]ds$$
$$+ \epsilon g_{\text{Na}}R_m\mu_o^2\eta_o\left(\frac{1 - e^{-\Phi_{\text{Na}}U_{\text{peak}}\Lambda}}{\lambda\,\Lambda}\right)\sum_{i=1}^{N}G_{pi}(T). \tag{16}$$

The subscripts correspond to the voltage response at location $X=X_p$ in the presence of a BAP at $X = X_0$ and hotspot locations at $X = X_i$. Let

$$\Gamma(\Phi) = \mu^2[\Phi]\eta[\Phi]\Phi\frac{(e^{(\Phi-\Phi_{\text{Na}})U_{\text{peak}}\Lambda} - 1)}{(e^{\Phi U_{\text{peak}}\Lambda]} - 1)} \tag{17}$$

and

$$\Psi_P(T) = \int_0^T\sum_{k=0}^{\mathcal{R}}\left(\frac{U(s)}{U_{\text{peak}}}\right)H(s - k\omega)G_{po}(T - s)ds$$
$$+ \epsilon g_{\text{Na}}R_m\mu_o^2\eta_o\left(\frac{1 - e^{-\Phi_{\text{Na}}U_{\text{peak}}\Lambda}}{\Lambda}\right)\sum_{i=1}^{N}G_{pi}(T), \tag{18}$$

then Eqn (16) becomes

$$\Phi_P(T) = \Psi_P(T)$$
$$+ \epsilon\left(\frac{g_{\text{Na}}R_m}{\lambda}\right)\int_0^T\sum_{i=1}^{N}\Gamma[\Phi_i(s)]G_{pi}(T - s)ds. \tag{19}$$

Equation (19) is our resulting nonlinear Volterra integral equation for the membrane potential (Φ) which can be solved using a number of different methods. However, here we have applied regular perturbation theory leading to a perturbation expansion that yields a sequence of linear Volterra integral equations.

5. A perturbative approach for the membrane potential

Let the depolarization be represented as a membrane potential perturbation from the passive BAP in the form of a perturbative expansion:

$$\Phi(X, T) = \Phi_0(X, T) + \sum_{v=1}^{\infty}\epsilon^v\Phi_v(X, T), \tag{20}$$

where $\Phi_v(X, T)$ is the perturbed voltage from the zero-order $\Phi_0(X, T)$ approximation given by solving Eqn. (14). On substituting our expansion Eqn (20) into Eqn (19) and equating coefficients of powers of system ϵ, a sequence of linear Volterra integral equations describing the nonlinear perturbations of the voltage from the passive cable voltage response $\Phi_o(X, T)$ is obtained via a Taylor expansion of Γ to yield up to $O(\epsilon^4)$:

$$\Phi_{1p}(T) =$$
$$g_{\text{Na}}\left(\frac{R_m}{\lambda}\right)\sum_{i=1}^{N}\int_0^T G_{pi}(T - s)\Gamma[\Phi_{oi}(s)]ds$$
$$+ g_{\text{Na}}\mu_o^2\eta_o\left[\frac{1 - e^{(-\Phi_{\text{Na}}U_{\text{peak}}\Lambda)}}{\Lambda}\right]G_{pi}(T)$$

$$\Phi_{2p}(T) =$$
$$g_{\text{Na}}\left(\frac{R_m}{\lambda}\right)\sum_{i=1}^{N}\int_0^T G_{pi}(T - s)\Gamma'[\Phi_{0i}(s)]\Phi_{1i}(s)ds$$

$$\Phi_{3p}(T) =$$
$$g_{Na}\left(\frac{R_m}{\lambda}\right)\sum_{i=1}^{N}\int_0^T G_{pi}(T-s)\left\{\Gamma'[\Phi_{0i}(s)]\,\Phi_{2i}(s)\right.$$
$$\left. + \frac{1}{2!}\Gamma''[\Phi_{0i}(s)]\,\Phi_{1i}^2(s)\right\}ds$$

$$\Phi_{4p}(T) =$$
$$g_{Na}\left(\frac{R_m}{\lambda}\right)\sum_{i=1}^{N}\int_0^T G_{pi}(T-s)\left\{\Gamma'[\Phi_{0i}(s)]\,\Phi_{3i}(s)\right.$$
$$+ \Gamma''[\Phi_{0i}(s)]\,\Phi_{1i}(s)\Phi_{2i}(s)$$
$$\left. + \frac{1}{3!}\Gamma'''[\Phi_{0i}(s)]\,\Phi_{1i}^3(s)\right\}ds,$$

where G is the Green's function.

6. Determining the sodium activation and inactivation in the current-clamp case.

The dimensionless activation (μ) and inactivation (η) reflect the opening and closing of a small cluster of Na^+ channels, respectively, whose dynamics follow reaction kinetics described by a first-order ordinary differential equation of the form (Hodgkin & Huxley, 1952):

$$(1/\tau_m)\frac{\partial \xi}{\partial T} = \alpha_\xi(\Phi)(1-\xi) - \beta_\xi(\Phi)\xi \tag{21}$$

or equivalently

$$(1/\tau_m)\frac{\partial \xi}{\partial T} = \frac{(\xi_\infty(\Phi) - \xi)}{\tau_\xi(\Phi)}, \tag{22}$$

where

$$\xi_\infty(\Phi) = \frac{\alpha_\xi(\Phi)}{\alpha_\xi(\Phi) + \beta_\xi(\Phi)}$$

and

$$\tau_\xi(\Phi) = \frac{1}{\alpha_\xi(\Phi) + \beta_\xi(\Phi)}.$$

Note that in some cases $\xi_\infty(\Phi)$ may be explicitly given by a functional form like

$$\xi_\infty(\Phi) = \frac{1}{1 + e^{(\Phi U_{peak} + E_R + b_\xi)/c_\xi}} \tag{23}$$

and the rate-constants (sec)$^{-1}$ are Boltzmann-type functions of the form:

$$\alpha_\xi(\Phi) = \frac{A_\alpha(\Phi U_{peak} + E_R - b_\alpha)}{1 - e^{-(\Phi U_{peak} + E_R - b_\alpha)/c_\alpha}}$$
$$\beta_\xi(\Phi) = \frac{A_\beta(\Phi U_{peak} + E_R - b_\beta)}{1 - e^{(\Phi U_{peak} + E_R - b_\alpha)/c_\beta}},$$

where a_α, b_α, c_α, a_β, b_β, c_β, b_ξ and c_ξ are constants. For example, based on experimental data obtained by Mainen et al. (1995) for neocortical dendrites, the parameters used to calculate the activation function were: $a_\alpha = 0.182$, $b_\alpha = -35.0$, $c_\alpha = 9.0$, $a_\beta = -0.124$, $b_\beta = -35.0$, $c_\beta = -9.0$ and for the inactivation function Eqn. (22) was used with Eqn. (23) where: $a_\alpha = 0.024$, $b_\alpha = -50.0$, $c_\alpha = 5.0$, $a_\beta = -0.0091$, $b_\beta = -75.0$, $c_\beta = -5.0$, $b_\xi = -65$ and $c_\xi = 6.2$.

Calculating the first-order correction term $\Phi_1(X, T)$ requires calculating the activation $\mu(\Phi_{0i})$ and inactivation $\eta(\Phi_{0i})$ gating variables for each hotspot location of the Na^+ channel, using the zero-order term $\Phi_0(X, T)$, the solution of the linear diffusion equation given by Eqn (14). Here, we used the channel descriptions given in Mainen et al. (1995), where the gating variables are given by:

$$(1/\tau_m)\frac{\partial \mu[\Phi_{0i}]}{\partial T} =$$
$$\alpha_\mu(\Phi_{0i})\big(1 - \mu[\Phi_{0i}]\big) - \beta_\mu(\Phi_{0i})\mu[\Phi_{0i}]$$
$$(1/\tau_m)\frac{\partial \eta[\Phi_{0i}]}{\partial T} = \frac{\eta_\infty(\Phi_{0i}) - \eta[\Phi_{0i}]}{\tau_\eta(\Phi_{0i})},$$

where $\eta_\infty(\chi) = 1/(1 + e^{(\chi U_{peak} + E_R + b_\xi)/c_\xi})$, $\tau_\eta(\chi) = 1/(\alpha_\eta(\chi) + \beta_\eta(\chi))$ and $\Phi_{0i} = \Phi_0(X_i,T)$. One must remember that the voltage term $\Phi(X,T)$ that would have appeared in the above equations has been replaced by the passive response $\Phi_0(X_i,T)$. For higher order correction terms ($n \geq 2$) of Φ, this involves derivative terms of the activation and inactivation functions with respect to the dimensionless voltage (Φ) evaluated at $\Phi = \Phi_{0i}$. These terms result from applying the perturbative expansion to all voltage-dependent terms in our system of equations, including the activation and inactivation terms of the Na^+ channels and equating terms in powers of ϵ. Here, we show the resulting expressions for activation variables described by Eqn. (21) one arrives at the following hierarchical systems of ordinary differential equations.

$$O(\varepsilon):$$
$$\frac{1}{\tau_m}\frac{\partial}{\partial T}\left(\Phi_{1i}\frac{\partial \xi[\Phi_{0i}]}{\partial \Phi_{0i}}\right) = \Phi_{1i}\frac{\partial \alpha_\xi[\Phi_{0i}]}{\partial \Phi_{0i}}$$
$$- \xi[\Phi_{0i}]\Phi_{1i}\left(\frac{\partial \alpha_\xi[\Phi_{0i}]}{\partial \Phi_{0i}} + \frac{\partial \beta_\xi[\Phi_{0i}]}{\partial \Phi_{0i}}\right)$$
$$- \big(\alpha_\xi[\Phi_{0i}] + \beta_\xi[\Phi_{0i}]\big)\left(\Phi_{1i}\frac{\partial \xi[\Phi_{0i}]}{\partial \Phi_{0i}}\right)$$
$$\tag{24}$$

$O(\varepsilon^2):$

$$\frac{1}{\tau_m}\frac{\partial}{\partial T}\left(\Phi_{2i}\frac{\partial\xi[\Phi_{0i}]}{\partial\Phi_{0i}}+\frac{1}{2}\Phi_{1i}^2\frac{\partial^2\xi[\Phi_{0i}]}{\partial\Phi_{0i}^2}\right)$$

$$=\Phi_{2i}\frac{\partial\alpha_\xi[\Phi_{0i}]}{\partial\Phi_{0i}}+\frac{1}{2}\Phi_{1i}^2\frac{\partial^2\alpha_\xi[\Phi_{0i}]}{\partial\Phi_{0i}^2}$$

$$-\Phi_{1i}\left(\frac{\partial\alpha_\xi[\Phi_{0i}]}{\partial\Phi_{0i}}+\frac{\partial\beta_\xi[\Phi_{0i}]}{\partial\Phi_{0i}}\right)\left(\Phi_{1i}\frac{\partial\xi[\Phi_{0i}]}{\partial\Phi_{0i}}\right)$$

$$-\left(\alpha_\xi[\Phi_{0i}]+\beta_\xi[\Phi_{0i}]\right)$$

$$\times\left(\Phi_{2i}\frac{\partial\xi[\Phi_{0i}]}{\partial\Phi_{0i}}+\frac{1}{2}\Phi_{1i}^2\frac{\partial^2\xi[\Phi_{0i}]i}{\partial\Phi_{0i}^2}\right)$$

$$-\xi[\Phi_{0i}]\left[\Phi_{2i}\left(\frac{\partial\alpha_\xi[\Phi_{0i}]}{\partial\Phi_{0i}}+\frac{\partial\beta_\xi[\Phi_{0i}]}{\partial\Phi_{0i}}\right)\right.$$

$$\left.+\frac{1}{2}\Phi_{1i}^2\left(\frac{\partial^2\alpha_\xi[\Phi_{0i}]}{\partial\Phi_{0i}^2}+\frac{\partial^2\beta_\xi[\Phi_{0i}]}{\partial\Phi_{0i}^2}\right)\right]$$

$$(25)$$

$O(\varepsilon^3):$

$$\frac{1}{\tau_m}\frac{\partial}{\partial T}\left(\Phi_{3i}\frac{\partial\xi[\Phi_{0i}]}{\partial\Phi_{0i}}+\Phi_{1i}\Phi_{2i}\frac{\partial^2\xi[\Phi_{0i}]}{\partial\Phi_{0i}^2}\right.$$

$$\left.+\frac{1}{6}\Phi_{1i}^3\frac{\partial^3\xi[\Phi_{0i}]}{\partial\Phi_{0i}^3}\right)$$

$$=\Phi_{3i}\frac{\partial\alpha_\xi i[\Phi_{0i}]}{\partial\Phi_{0i}}+\Phi_{1i}\Phi_{2i}\frac{\partial^2\alpha_\xi[\Phi_{0i}]}{\partial\Phi_{0i}^2}$$

$$+\frac{1}{6}\Phi_{1i}^3\frac{\partial^3\alpha_\xi[\Phi_{0i}]}{\partial\Phi_{0i}^3}$$

$$-\Phi_{1i}\left(\frac{\partial\alpha_\xi[\Phi_{0i}]}{\partial\Phi_{0i}}+\frac{\partial\beta_\xi[\Phi_{0i}]}{\partial\Phi_{0i}}\right)$$

$$\times\left(\Phi_{2i}\frac{\partial\xi[\Phi_{0i}]}{\partial\Phi_{0i}}+\frac{1}{2}\Phi_{1i}^2\frac{\partial^2\xi[\Phi_{0i}]}{\partial\Phi_{0i}^2}\right)$$

$$-\left[\Phi_{2i}\left(\frac{\partial\alpha_\xi[\Phi_{0i}]}{\partial\Phi_{0i}}+\frac{\partial\beta_\xi[\Phi_{0i}]}{\partial\Phi_{0i}}\right)\right.$$

$$\left.+\frac{1}{2}\Phi_{1i}^2\left(\frac{\partial^2\alpha_\xi[\Phi_{0i}]}{\partial\Phi_{0i}^2}+\frac{\partial^2\beta_\xi[\Phi_{0i}]}{\partial\Phi_{0i}^2}\right)\right]$$

$$\times\left(\Phi_{1i}\frac{\partial\xi[\Phi_{0i}]}{\partial\Phi_{0i}}\right)$$

$$-\left(\alpha_\xi[\Phi_{0i}]+\beta_\xi[\Phi_{0i}]\right)\left(\Phi_{3i}\frac{\partial\xi[\Phi_{0i}]}{\partial\Phi_{0i}}\right.$$

$$\left.+\Phi_{1i}\Phi_{2i}\frac{\partial^2\xi[\Phi_{0i}]}{\partial\Phi_{0i}^2}+\frac{1}{6}\Phi_{1i}^3\frac{\partial^3\xi[\Phi_{0i}]}{\partial\Phi_{0i}^3}\right)$$

$$-\xi[\Phi_{0i}][\Phi_{0i}]\left[\Phi_{3i}\left(\frac{\partial\alpha_\xi[\Phi_{0i}]}{\partial\Phi_{0i}}+\frac{\partial\beta_\xi[\Phi_{0i}]}{\partial\Phi_{0i}}\right)\right.$$

$$+\Phi_{1i}\Phi_{2i}\left(\frac{\partial^2\alpha_\xi[\Phi_{0i}]}{\partial\Phi_{0i}^2}+\frac{\partial^2\beta_\xi[\Phi_{0i}]}{\partial\Phi_{0i}^2}\right)$$

$$\left.+\frac{1}{6}\Phi_{1i}^3\left(\frac{\partial^3\alpha_\xi[\Phi_{0i}]}{\partial\Phi_{0i}^3}+\frac{\partial^3\beta_\xi[\Phi_{0i}]}{\partial\Phi_{0i}^3}\right)\right]$$

$$(26)$$

For activation/inactivation variables given by Eqn. (22) the hierarchy of equations resulting from perturbation is left as an exercise for the reader. Other potential interest methods are applying some transformation techniques similar to those used to solve Volterra integral equations (see Evans & Shenk, 1970; Mascagni, 1989).

7. Results

The first question of our investigation was to see how the nonlinear sodium current sources modify the passive response of our cable to the spike voltage clamp. **Fig 2** illustrates the passive BAP generated using Eqn (18).
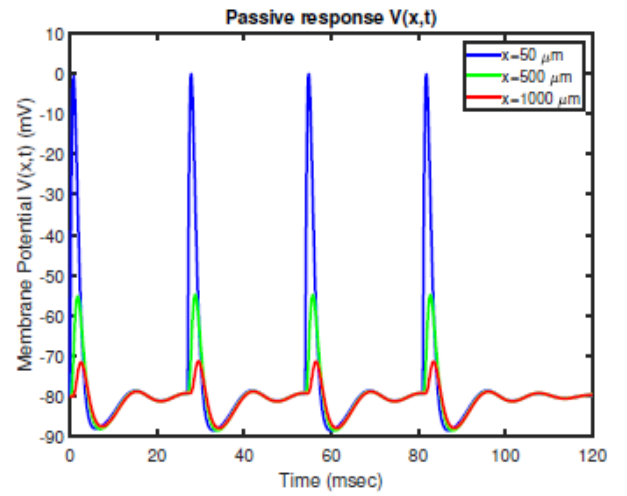
Figure 2: The passive response for our somatically injected voltage clamp for generating the backpropagating action potential recorded at locations x = 50μm, x = 500μm, and x = 1000μm along our cable.

Fig 3 illustrates how even a small number of Na+ hotspots can amplify the voltage response along the cable. The resulting amplification of the BAPs was generated from expression Eqn (20) at several locations along the cable of (dimensional) length L = 1000 μm and diameter d = 4μm, and uniform spatial distribution of hotspots from X = 0 to X = L located at length intervals of jL/N where j =1, 2,... .N.

In **Fig 4,** an identical number of hotspots but a non-identical number of Na+ channels per hotspot is considered. Specifically, we considered both a linearly increasing and decreasing number of Na+ of sodium channels per hotspot as a function of distance. **Fig 4** illustrates the voltage response at the same three locations used before. The results indicate that the
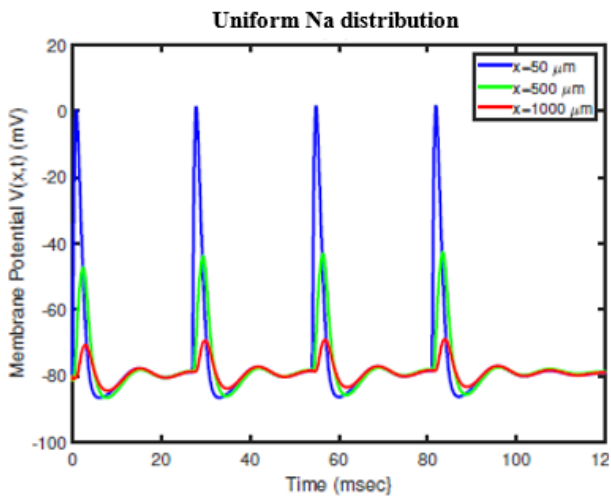
Figure 3: The voltage response for our somatically generated back propagating action potential in the presence of a uniform distribution of Na$^+$ channels and recorded at the same locations along our cable x = 50μm, x = 500μm, and x = 1000μm as those used for the passive response. Here, upon comparing with Fig 2, one can see that for a uniform distribution of 10 Na$^+$ channel hotspots can amplify the voltage response when compared with the passive response.
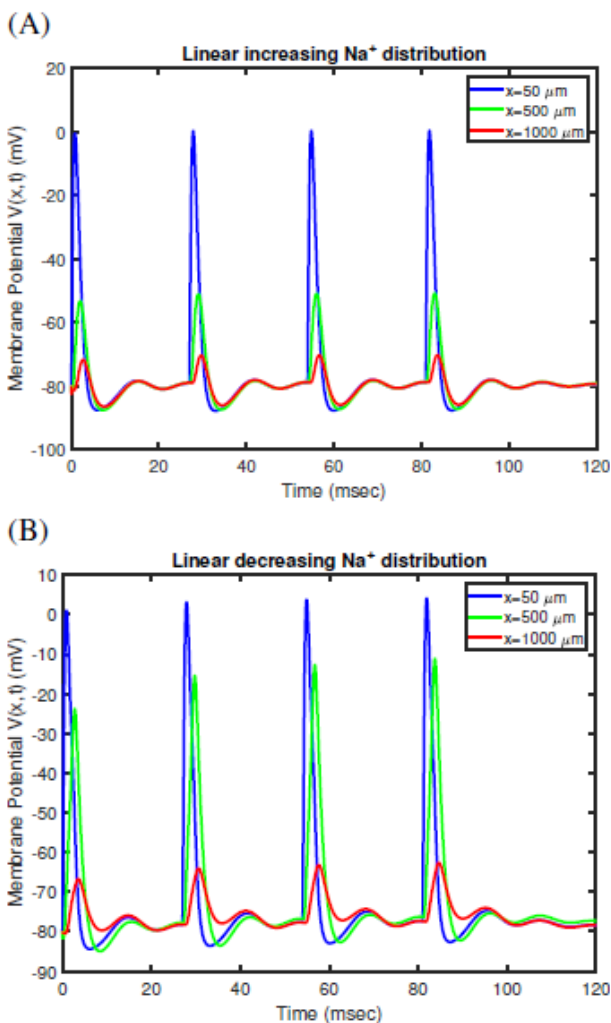

Figure 4: The voltage response at x = 50μm, x = 500μm, and x = 1000μm for (A) a linearly increasing and (B) a linearly decreasing Na$^+$ channel density as a function of distance from the soma.

Na$^+$ channels to exert an effect at various membrane potential levels in accordance with the I_{Na}−V dynamics. Hence, for large voltage excursions, the solution will also be affected by the strength of the inward current.

Fig 4 also presents an initially counterintuitive nonlinear effect on the resulting membrane potential, namely, as the number of Na$^+$ ion channels increase as a function of distance, one would expect that the maximum voltage of the BAP would also increase along the cable, and likewise with decreasing numbers of s Na$^+$ ion channels per hotspot as a function of distance, would result in less amplification of the membrane voltage. **Fig 4** does not indicate this. Instead, for the linear decreasing case, one can see greater amplification of the BAP at larger distances from the soma compared to the linearly increasing case. Why is this happening? The reason is the details of the Na$^+$ channel densities used in these simulations.

For the linearly increasing case, the number of Na$^+$ channels start associated with our default ion channel density of 100 pS/μm^2 and increases 10-fold when x = 1000 μm, while for the decreasing case, this same distribution is flipped (along the cable) so that at Na$^+$ channel density is 10 times higher at x = 0 μm and decreases linearly to default value at x = 1000 μm (1/10th the value at x = 0 μm). Here, it becomes apparent that, for the linearly decreasing distribution, the aggregate degree of boosting by the hotspots of the BAP along the cable is greater than the linearly increasing case since, for the linearly decreasing case, the channel density per hotspot is larger over the first half of the cable (from x = 0 to x = 500 μm), thereby resulting in larger amplification and better support of the BAP along the cable's extent. Moreover, the above results indicate that several factors influence how Na+ channels affect the BAP, including channel density and spatial distribution, the number of hotspots, and the distance between hotspots.

We wanted to observe how the BAP signal is amplified due to an additional number of hotspots or variations in the number of channels per unit length. We assume there are θ*(X$_i$) Na$^+$ channels that occupy each hotspot, where N*(X$_i$) = θ(X$_i$)/πd denotes the number of channels per unit length. Fig 5 illustrates how increasing the channel density per unit length (by increasing channel density per unit area) alters and amplifies the BAP along the cable. We observe moderate amplification of the BAP signal along the cable in **Fig 5A** but great amplification in **Fig 5B**.

The number of hotspots and the distance between hotspots or the inter-hotspot distance can also affect the amplitude and, to a lesser extent, the form of the BAP signal. We varied the number of hotspots by systematically increasing the number of hotspots from N = 20 to N = 80 (in steps of 20). We investigated the response by computing expression Eqn (20) for a cable of length L = 1000 μm and diameter d = 4μm, again assuming a uniform distribution of hotspots from X = 0 to X = L located at length intervals of jL/N. The results presented in **Fig 6** illustrate that an increased number of hotspots, along with a decrease in the inter-hotspot distance, leads to an increase in the amplitude of the BAP as it propagates along the cable.
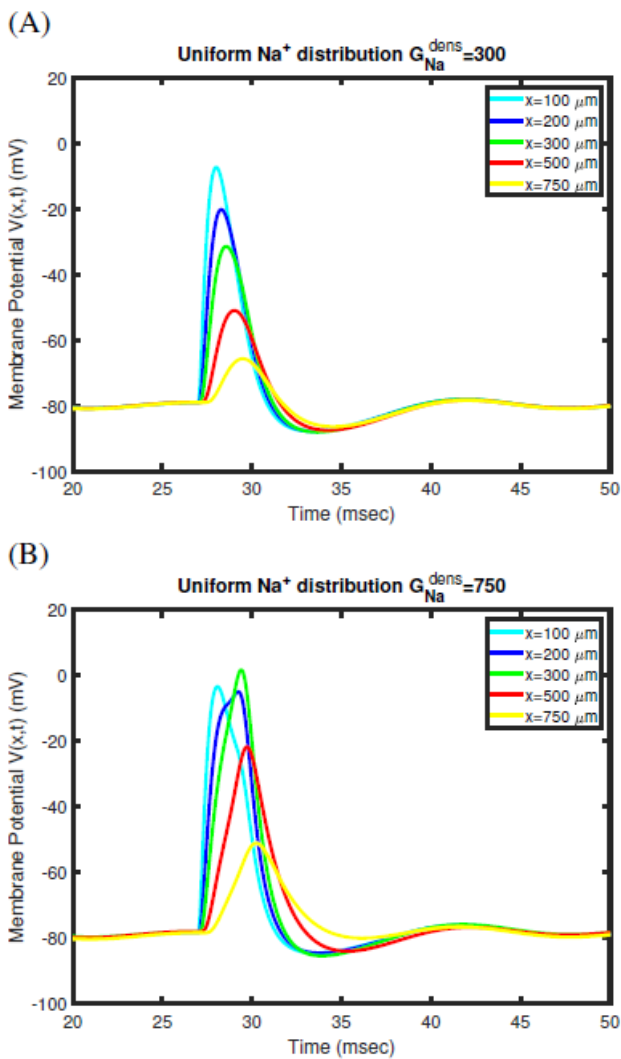

(A)

(B)

Figure 5: The BAP recorded at locations x = 100μm, x = 200μm, x = 300μm, x = 500μm, and x = 750μm for a Na+ channel density of (A) G_{Na} =300 pS/μm^2 and for (B) G_{Na} =750 pS/μm^2

(A)

(B)

(C)

(D)
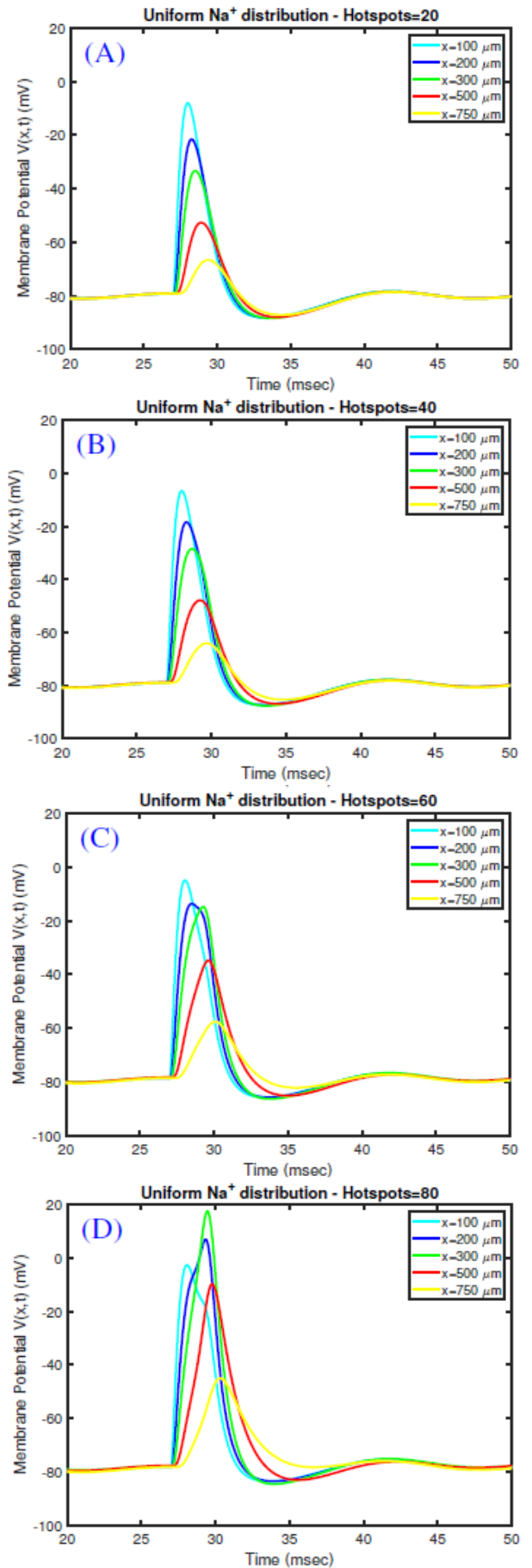
Figure 6: The BAP recorded at locations x = 100μm, x = 200μm, x = 300μm, x = 500μm, and x = 750μm for increasing number of hotspots Na$^+$ channel density of (A) N = 20 (B) N = 40 (C) N = 60 and (D) N = 80 hotspots

The ionic cable equation in its full and unexpanded form is a nonlinear system of equations, and thus it can be expected to have several behaviors ranging from complex, chaotic attractors and resonances to simpler stationary states, periodic orbits, solitary waves and limit cycles; complex behavior in particular, can be expected when periodic forcing terms are present. In order to study the nonlinear behavior analytically, we have resorted to a regular perturbative expansion concerning the voltage to derive a set of expressions that describe how the passive voltage is altered according to these perturbative terms. Here, the resulting terms of the expansion can be viewed as a quasilinear approach toward understanding how the passive response is transformed. However, one must know potential convergence issues caused by insufficient terms.

It would be interesting to see whether one can find an optimum number and distribution of Na^+ channels that preserves the maximum amplitude of the BAP while it propagates along the extent of the cable. The hotspots would essentially need to support a form of quasi-saltatory propagation and, in principle, would require each hotspot and its constituent Na^+ channels to operate with optimal conductance as allowed by the $I_{Na}-V$ dynamics to achieve maximum propagation. By increasing the number of Na^+ channels per hotspot ($\theta*$) via the conductance g_{Na}, a relatively small number of hotspots would be required to produce sufficient amplification of the BAP signal and provide one with the means to yield an optimal number of Na^+ channels. On the other hand, by decreasing the conductance g_{Na}, more hotspots will be required to preserve the amplitude (and, to a lesser extent, the shape) of the BAP during transit along the spatial extent of the cable under investigation. When increasing the number of hotspots, one needs to remember that too many hotspots will lead to large deviations in the profile of the calculated voltage. Here, one needs to optimize both the strength of the channels that make up the hotspot, the distribution of hotspots, as well as the inter-hotspot interval (the distance between hotspots) in a way that may likely require one to adopt a conservation rule where doubling the number of hotspots will require each hotspot to generate half the current. This assumption is a natural consequence of conserving generated current, but the actual method is likely not as simple since each hotspot should boost the passive response just enough to generate a realistic BAP.

8. Discussion

An *a priori* assumption of the theory is that Na^+ channels along the dendritic axis are far less abundant than those found along the somatoaxonal axis and in discrete patches resembling hotspots. This assumption is based on the nature of ion channels being pores embedded in the neuron's membrane (Hille, 2001), suggesting that ion channels are distributed discretely. Still, this assumption can be made as general as we like by reducing the distance between hotspots to approximate a continuous layer of ionic channels. Significantly, further studies have provided additional evidence that ion channels are discretely distributed in neuronal dendrites, and an increasing body of experimental literature that supports the ion channels tend to form clusters occupying finite domains or hotspots along the dendrite's plasma membrane (Ballou et al., 2006; Lai & Jan, 2006; McKeown et al., 2008; Misonou & Trimmer, 2004; Sheng et al., 1992; Trimmer & Rhodes, 2004) however, the underlying mechanisms for the locations and discrete nature of such ion channel distributions needs further experimental investigation.

The passive membrane time-constant $\tau_m = R_m C_m$ is calculated from values of the membrane resistivity (R_m) as the membrane capacitance (C_m) is a fixed constant of $1\mu F/cm^2$. R_m is an intrinsic property of the receptor membrane. Since synaptic receptors are located peripherally, it suggests that R_m is low in distal dendrites. A favorable fit to a compartment model has been a sigmoidally decreasing function for neocortical pyramidal dendrites to a final value of $R_m = 5357 \ \Omega cm^2$ (Stuart & Spruston, 1998). However, notwithstanding the problems inherent in such neural modeling protocols for active properties of the dendritic membrane, *in vitro,* preparations are unlikely to be appropriate for values encountered *in vivo*. The significance of even lower $R_m \approx 500 \ \Omega cm^2$ used by Chiu et al. (1979) for myelinated axons in comparison to $R_m \approx 3300 \ \Omega cm^2$ or a leakage conductance of $0.3 \ mS/cm^2$ used by Hodgkin & Huxley (1952) for an unmyelinated axon membrane is in line with the value used by early investigators of the passive dendritic properties of CNS neurons (e.g., Rall (1959)). This would be advantageous to a highly modulatory environment of the dendritic neuropil *in vivo* due to a highly rich receptor-covered membrane arising both synaptically and extrasynaptically (Aiello & Bach-y Rita, 1997).

FitzHugh (1960) first studied reduced systems of equations when one or more gating variables were held constant. A reduced system, in which only the K⁺ activation was held constant at the resting value, was shown to result in the action potential not returning to rest but maintaining an infinite plateau potential. FitzHugh (1960) remarked that such an approach could not yield sufficient information to explain how trains of action potentials can be modeled with H-H equations. In other words, it fails to qualitatively reproduce the pulse recovery necessary for repeated firing or trains of BAPs. Holden and colleagues, in a series of papers (see Holden,1980, 1981; Holden & Winlow,1983), have shown that specific changes in K⁺ channel density can lead to autorhythmicity: excitable membranes that lack K⁺ channels are stabilized by a high leakage conductance (or low R_m).

The H-H equations exhibit a wide variety of dynamical activity, ranging from oscillations (Taylor et al., 1995) and periodic orbits (Troy, 1977) to complex chaotic behavior (Maršalek & Santamarıa, 1998). Changes to the K⁺ channel density in the H-H membrane can lead to small amplitude oscillations investigated mathematically by Taylor et al. (1995) and large amplitude periodic solutions that reflect a repetitive discharge of action potentials investigated mathematically by Troy (1977). As a result, a Na⁺ pump and/or Na⁺−Ca²⁺ exchanger current is included in the model. It should be mentioned that all calcium (Ca²⁺) currents are not involved in generating repetitive action potentials because action potentials can be generated in the presence of calcium antagonists, such as Co²⁺ or Cd²⁺ when added to the bath solution, in the experiment. So we avoided the complication of a Na⁺ − Ca²⁺ exchanger in the model, although modeling of induced Ca²⁺ influx as a result of BAPs has been done with compartmental modeling (Maršalek & Santamarıa, 1998). Nevertheless, experimental results show that single BAP causes an influx of Ca²⁺ (e.g., Jaffe et al.,1992; Markram et al., 1995; Xiong & Chen, 2002).

The H-H equations exhibit repetitive firing, typically when stimulated by suprathreshold constant input leading to infinite trains of APs and the case of nonlinear cables, infinite trains of BAPs, yet experiments show finite trains of BAPs. The slow inactivation process would account for this discrepancy (e.g., Fleidervish et al., 1996). Decremental conduction of the BAP could also result from a large amount of K⁺ ions in the external medium. Despite this, the Hoffman et al. (1997) model of peak reduction of BAPs due to a high concentration

of K⁺ channels in distal dendrites are one mechanism for the decremental conduction of the BAP. However, there are concerns about the validity of this since experiments indicating that K⁺ channels are discretely distributed in dendrites (Ballou et al., 2006; McKeown et al., 2008; Misonou &Trimmer, 2004; Trimmer & Rhodes, 2004) and because of the cost of maintaining a high and continuous density distribution of K⁺ channels is high, requiring metabolic energy to transport from the soma to such terminal dendrites an enzyme for catasynthesis of the protein during endocytosis. Despite this, the inclusion of calcium (diffusion) dynamics along with a Na⁺ pump and/or Na⁺−Ca²⁺ exchanger, A-type K⁺ currents (Hoffman et al., 1997; Migliore et al., 1999), and nonspecific cation currents (Magee, 1998; Migliore, 2003) modulates the spatiotemporal spread of BAPs during synaptic integration.

9. Conclusion

In the last decade, we have seen a rapid rise in computational models but limited recourse to the further development of nonlinear cable theory (Iannella et al., 2014; Poznanski et al., 2017a, b). Apart from a new cable theory based on the path integral developed because compartmental models are considered to be inappropriate since they do not provide a continuous description of the membrane potential as a function of space (position) and time but rather a discrete approximation to it (see Cao & Abbott, 1993).

Few advances have been made beyond what was known four decades ago, as summarized in the monograph by (Jack et al., 1983, (on p. 305)): "*Although subthreshold oscillatory activity may be treated semi-analytically using the equations for the time dependence of the ionic current given by Hodgkin-Huxley (see Sabah & Leibovic (1969)), it is more difficult to analyze oscillator activity in response to larger currents near or beyond the threshold for initiating action potentials. If the Hodgkin-Huxley and cable equations are used, it is necessary to resort almost entirely to numerical computations*'." Nevertheless, we have advanced analytical models of active propagation in dendrites well beyond what was known two decades ago.

Analytical solutions of the H-H equations for a suprathreshold input representation of a BAP at a point close to the soma were found for a dendrite model containing transient Na⁺ channels spatially distributed at discrete locations along the dendritic

axis. This investigation highlights that analytical approaches can be developed to tackle difficult nonlinear problems.

Conflict of Interest

The authors declare no conflict of interest.

Appendix

The following integral for $\Phi_0(X,T)$ needs to be evaluated, representing the solution to the linear cable equation:

$$\Phi_0(X, T) = \int_0^T \frac{I_A(0, T - s)}{U_{peak}} G(X, 0; s)\,ds$$

where

$$I_A(0, T) = U_o\left\{ \sin\left(\frac{2\pi}{5}T\right)e^{-0.2\mathcal{A}T} \right.$$
$$\left. + 150e^{-2\mathcal{A}T} - 100e^{-4\mathcal{A}T} - 50e^{-1.2\mathcal{A}T} \right\}H(T),$$

where $\mathcal{A} = 15$, $H(T)$ is the Heaviside step function, and $G(X,0;T)$ is the Green's function given by the solution to the following initial value problem:

$$\frac{\partial G}{\partial T}(X, 0; T) =$$
$$\frac{\partial^2 G}{\partial X^2}(X, 0; T) - G(X, 0; T) + \delta(X)\delta(T), \quad T > 0$$
$$G(X, 0; 0) = 0$$

and corresponds to the response at time T at position X to a unit impulse at $X = 0$ and $T = 0$. For a finite cable with a killed-end boundary condition $G(0, 0; T) = 0$ at $X = 0$ and a sealed-end condition $\partial G(L, 0, T)/\partial X = 0$ at $X = L$, several representations for the Green's function converges for small and large T (Tuckwell, 1988). Here we have used the following expression for $G(X,0;T)$ that converges for small T values:

$$G(X, 0; T) = \frac{e^{-T}}{\sqrt{4\pi T^3}} \sum_{n=0}^{\infty} (-1)^n \left\{ \right.$$
$$[2(n + 1)L - X]\exp\left(-\frac{[2(n + 1)L - X]^2}{4T}\right)$$
$$\left. + [2nL + X]\exp\left(-\frac{[2nL + X]^2}{4T}\right)\right\},$$
$$T > 0,\ 0 < X < L$$

and the one for $G(X, X_i; T)$ for is calculated from

$$\frac{\partial G}{\partial T}(X, X_i; T) =$$
$$\frac{\partial^2 G}{\partial X^2}(X, X_i; T) - G(X, X_i; T) + \delta(X - X_i)\delta(T),$$
$$T > 0$$
$$G(X, X_i; 0) = 0$$

with the following killed-end boundary condition $G(0, X_i; T) = 0$ at $X = 0$ and sealed-end condition $\partial G(L, X_i, T)/\partial X = 0$ at $X = L$ (where L is the electrotonic length) is expressed as:

$$G(X, X_i; T) = H(X_i - X)\left[\vphantom{\frac{(X)^2}{4T}}\right.$$

$$\exp\left(-\frac{(X - X_i)^2}{4T}\right) - \exp\left(-\frac{(X + X_i)^2}{4T}\right)$$
$$+ \exp\left(-\frac{(X + X_i - 2L)^2}{4T}\right) - \exp\left(-\frac{(X - X_i + 2L)^2}{4T}\right)$$
$$- \exp\left(-\frac{(X - X_i - 2L)^2}{4T}\right)$$
$$+ \exp\left(-\frac{(X + X_i + 2L)^2}{4T}\right)$$
$$- \exp\left(-\frac{(X - X_i - 2L)^2}{4T}\right)$$
$$+ \exp\left(-\frac{(X + X_i + 2L)^2}{4T}\right)$$
$$+ \exp\left(-\frac{(X - X_i + 4L)^2}{4T}\right)$$
$$- \exp\left(-\frac{(X + X_i - 4L)^2}{4T}\right)$$
$$+ \exp\left(-\frac{(X - X_i - 4L)^2}{4T}\right)$$
$$- \exp\left(-\frac{(X + X_i + 4L)^2}{4T}\right)$$
$$+ \exp\left(-\frac{(X + X_i - 6L)^2}{4T}\right)$$
$$- \exp\left(-\frac{(X - X_i + 6L)^2}{4T}\right)$$
$$- \exp\left(-\frac{(-X + 3X_i)^2}{4T}\right) + \exp\left(-\frac{(X + 3X_i)^2}{4T}\right)$$

$$+ 2\exp\left(-\frac{(-X + X_i + 4L)^2}{4T}\right)$$
$$- 2\exp\left(-\frac{(X + X_i + 4L)^2}{4T}\right)$$
$$+ 2\exp\left(-\frac{(-X + 3X_i + 2L)^2}{4T}\right)$$
$$- 2\exp\left(-\frac{(X + X_i + 2L)^2}{4T}\right)$$
$$+ \exp\left(-\frac{(-X + X_i + 2L)^2}{4T}\right)$$
$$- \exp\left(-\frac{(X + 7X_i + 2L)^2}{4T}\right)$$
$$+ \exp\left(-\frac{(-X + 5X_i)^2}{4T}\right) - \exp\left(-\frac{(X - 7X_i)^2}{4T}\right)\right]$$

$$\mathcal{H}(X, X_i; T) = H(X - X_i)\left[\vphantom{\frac{X}{T}}\right.$$

$$\exp\left(-\frac{(x-y)^2}{4T}\right) - \exp\left(-\frac{(x+y)^2}{4T}\right)$$

$$+\exp\left(-\frac{(x+y-2L)^2}{4T}\right) - \exp\left(-\frac{(x-y-2L)^2}{4T}\right)$$

$$-\exp\left(-\frac{(x-y+2L)^2}{4T}\right) + \exp\left(-\frac{(x+y+2L)^2}{4T}\right)$$

$$-\exp\left(-\frac{(x-y+2L)^2}{4T}\right) + \exp\left(-\frac{(x+y+2L)^2}{4T}\right)$$

$$-\exp\left(-\frac{(x+y-4L)^2}{4T}\right) + \exp\left(-\frac{(x-y-4L)^2}{4T}\right)$$

$$-\exp\left(-\frac{(x+y+4L)^2}{4T}\right) + \exp\left(-\frac{(x-y+4L)^2}{4T}\right)$$

$$+\exp\left(-\frac{(x+y-6L)^2}{4T}\right) - \exp\left(-\frac{(x-y-6L)^2}{4T}\right)$$

$$-\exp\left(-\frac{(3x-y)^2}{4T}\right) + \exp\left(-\frac{(3x+y)^2}{4T}\right)$$

$$+2\exp\left(-\frac{(x-y+4L)^2}{4T}\right)$$

$$+2\exp\left(-\frac{(3x-y+2L)^2}{4T}\right)$$

$$-2\exp\left(-\frac{(x+y+4L)^2}{4T}\right)$$

$$-2\exp\left(-\frac{(3x+y+2L)^2}{4T}\right)$$

$$+\exp\left(-\frac{(3x-y+2L)^2}{4T}\right) + \exp\left(-\frac{(5x-y)^2}{4T}\right)$$

$$-\exp\left(-\frac{(7x+y+2L)^2}{4T}\right) - \exp\left(-\frac{(-7x+y)^2}{4T}\right)\Bigg]$$

$$G(X, X_i; T) = \frac{e^{-T}}{\sqrt{4\pi T}}\Big[\mathcal{G}(X, X_i; T) + \mathcal{H}(X, X_i; T)\Big]$$

respectively.

The integral expression for $\Phi_0(X, T)$ can be solved analytically but requires the following integrals to be used,

$$\Gamma\left(-n-v-1; \frac{X^2}{4T}\right) = \int_{\frac{X^2}{4T}}^{\infty} z^{-v-2-n}\exp(-z)dz,$$

$$I = \int_0^T \zeta^v \exp\left(\zeta(\alpha-1) - \frac{X^2}{4\zeta}\right)d\zeta,$$

$$\Phi_0(X, T) = \frac{U_0}{\sqrt{\pi}U_{peak}}\Bigg[e^{-0.2\mathcal{A}T}\sin\left(\frac{2}{5}\pi\mathcal{A}T\right)$$

$$\times \sum_{n=0}^{\infty}\sum_{\ell=0}^{\infty}\sum_{p=0}^{\infty}\frac{(-1)^{n+\ell}}{(2\ell)!p!}\left(\frac{[2(n+1)L-X]^2}{4}\right)^{2\ell+p}$$

$$\times (0.2\mathcal{A}-1)^p$$

$$\times \Gamma\left(-2\ell-p+\frac{1}{2}; \frac{[2(n+1)L-X]^2}{4T}\right)\Bigg]H(T)$$

$$-\frac{U_0}{\sqrt{\pi}U_{peak}}\Bigg[e^{-0.2\mathcal{A}T}\cos\left(\frac{2}{5}\pi\mathcal{A}T\right)$$

$$\times \sum_{n=0}^{\infty}\sum_{\ell=0}^{\infty}\sum_{p=0}^{\infty}\frac{(-1)^{n+\ell}}{(2\ell+1)!p!}\left(\frac{[2(n+1)L-X]^2}{4}\right)^{2\ell+p}$$

$$\times (0.2\mathcal{A}-1)^p$$

$$\times \Gamma\left(-2\ell-p-\frac{1}{2}; \frac{[2(n+1)L-X]^2}{4T}\right)\Bigg]H(T)$$

$$+\frac{U_0}{\sqrt{\pi}U_{peak}}\Bigg[e^{-0.2\mathcal{A}T}\sin\left(\frac{2}{5}\pi\mathcal{A}T\right)$$

$$\times \sum_{n=0}^{\infty}\sum_{\ell=0}^{\infty}\sum_{p=0}^{\infty}\frac{(-1)^{n+\ell}}{(2\ell)!p!}\left(\frac{[2nL+X]^2}{4}\right)^{2\ell+p}$$

$$\times (0.2\mathcal{A}-1)^p$$

$$\times \Gamma\left(-2\ell-p+\frac{1}{2}; \frac{[2nL+X]^2}{4T}\right)\Bigg]H(T)$$

$$-\frac{U_0}{\sqrt{\pi}U_{peak}}\Bigg[e^{-0.2\mathcal{A}T}\cos\left(\frac{2}{5}\pi\mathcal{A}T\right)$$

$$\times \sum_{n=0}^{\infty}\sum_{\ell=0}^{\infty}\sum_{p=0}^{\infty}\frac{(-1)^{n+\ell}}{(2\ell+1)!p!}\left(\frac{[2nL+X]^2}{4}\right)^{2\ell+p}$$

$$\times (0.2\mathcal{A}-1)^p$$

$$\times \Gamma\left(-2\ell-p-\frac{1}{2}; \frac{[2nL+X]^2}{4T}\right)\Bigg]H(T)$$

$$+\frac{50U_0}{\sqrt{\pi}U_{peak}}\sum_{n=0}^{\infty}\sum_{p=0}^{\infty}(-1)^n\frac{[2(n+1)L-X]^{2p}}{p!}$$

$$\times \Gamma\left(-p+\frac{1}{2}; \frac{[2(n+1)L-X]^2}{4T}\right)$$

$$\times \left[3\frac{(2\mathcal{A}-1)^p}{4}e^{-2\mathcal{A}T} - 2\frac{(4\mathcal{A}-1)^p}{4}e^{-4\mathcal{A}T}\right.$$

$$\left. - \frac{(1.2\mathcal{A}-1)^p}{4}e^{-1.2\mathcal{A}T}\right]H(T)$$

$$+\frac{50U_0}{\sqrt{\pi}U_{peak}}\sum_{n=0}^{\infty}\sum_{p=0}^{\infty}(-1)^n\frac{[2nL+X]^{2p}}{p!}\times$$

$$\Gamma\left(-p+\frac{1}{2}; \frac{[2nL+X]^2}{4T}\right)\left[3\frac{(2\mathcal{A}-1)^p}{4}e^{-2\mathcal{A}T}\right.$$

$$\left. - 2\frac{(4\mathcal{A}-1)^p}{4}e^{-4\mathcal{A}T} - \frac{(1.2\mathcal{A}-1)^p}{4}e^{-1.2\mathcal{A}T}\right]H(T)$$

Now keeping the terms for positive integers k = 0 and p = 0, 1 and utilizing the following identities

$$\Gamma\left(\frac{1}{2}; \frac{X^2}{4T}\right) = \sqrt{\pi}\, Erfc\left(\frac{X}{\sqrt{4T}}\right)$$

$$\Gamma\left(-\frac{1}{2}; \frac{X^2}{4T}\right) = \frac{4\sqrt{T}}{X}\, exp\left(\frac{X^2}{4T}\right) - 2\sqrt{\pi}\, Erfc\left(\frac{X}{\sqrt{4T}}\right)$$

leads to the following expression for $\Phi_0(X, T)$ used in all the simulations:

$$\Phi_0(X,T) = \frac{U_0}{\sqrt{\pi}U_{peak}}\sum_{n=0}^{\infty}(-1)^n e^{-0.2\mathcal{A}T}\Bigg\{$$

$$\sin\left(\frac{2}{5}\pi\mathcal{A}T\right)\sqrt{\pi}Erfc\left(\frac{[2(n+1)L-X]}{2\sqrt{T}}\right)$$

$$+ \sin\left(\frac{2}{5}\pi\mathcal{A}T\right)\Bigg[(0.2\mathcal{A}-1)[2(n+1)L-X]$$

$$\times \sqrt{T}exp\left(-\frac{[2(n+1)L-X]^2}{4T}\right)$$

$$- (0.2\mathcal{A}-1)\left(\frac{[2(n+1)L-X]^2)}{4}\right)\sqrt{T}$$

$$\times 2\sqrt{\pi}Erfc\left(\frac{[2(n+1)L-X]}{2\sqrt{T}}\right)\Bigg]$$

$$- \cos\left(\frac{2}{5}\pi\mathcal{A}T\right)\left(\frac{[2(n+1)L-X]^2}{4}\right)$$

$$\times \sqrt{\pi}Erfc\left(\frac{[2(n+1)L-X]}{2\sqrt{T}}\right)$$

$$- \cos\left(\frac{2}{5}\pi\mathcal{A}T\right)(0.2\mathcal{A}-1)\left(\frac{[2(n+1)L-X]^3}{4}\right)$$

$$\times \sqrt{T}exp\left(-\frac{[2(n+1)L-X]^2}{4T}\right)$$

$$+ \cos\left(\frac{2}{5}\pi\mathcal{A}T\right)(0.2\mathcal{A}-1)\left(\frac{[2(n+1)L-X]^2}{4}\right)^2$$

$$\times 2\sqrt{\pi}Erfc\left(\frac{[2(n+1)L-X]}{2\sqrt{T}}\right)$$

$$+ \sin\left(\frac{2}{5}\pi\mathcal{A}T\right)\sqrt{\pi}Erfc\left(\frac{[2nL+X]}{2\sqrt{T}}\right)$$

$$+ \sin\left(\frac{2}{5}\pi\mathcal{A}T\right)\Bigg[(0.2\mathcal{A}-1)$$

$$+ \frac{50U_0}{\sqrt{\pi}U_{peak}}\Bigg\{4[2(n+1)L-X]\sqrt{T}$$

$$\times exp\left(\frac{[2(n+1)L-X]^2}{4T}\right)\Bigg[3\cdot\frac{(2\mathcal{A}-1)}{4}e^{-2\mathcal{A}T}$$

$$- 2\frac{(4\mathcal{A}-1)}{4}e^{-4\mathcal{A}T} - \frac{(1.2\mathcal{A}-1)}{4}e^{-1.2\mathcal{A}T}\Bigg]$$

$$+ \sqrt{\pi}Erfc\left(\frac{[2(n+1)L-X]}{\sqrt{4T}}\right)$$

$$\times \Bigg[\left(3 - 6\frac{(2\mathcal{A}-1)}{4}[2(n+1)L-X]^2\right)e^{-2\mathcal{A}T}$$

$$- \left(2 - 4\frac{(4\mathcal{A}-1)}{4}[2(n+1)L-X]^2\right)e^{-4\mathcal{A}T}$$

$$- \left(1 - 2\frac{(1.2\mathcal{A}-1)}{4}[2(n+1)L-X]^2\right)$$

$$\times e^{-1.2\mathcal{A}T}\Bigg]\Bigg\}H(T)$$

$$+ \frac{50U_0}{\sqrt{\pi}U_{peak}}\Bigg\{4[2nL+X]\sqrt{T}exp\left(\frac{[2nL+X]^2}{4T}\right)$$

$$\times \Bigg[3\frac{(2\mathcal{A}-1)}{4}e^{-2\mathcal{A}T} - 2\frac{(4\mathcal{A}-1)}{4}e^{-4\mathcal{A}T}$$

$$- \frac{(1.2\mathcal{A}-1)}{4}e^{-1.2\mathcal{A}T}\Bigg] + \sqrt{\pi}Erfc\left(\frac{[2nL+X]}{\sqrt{4T}}\right)$$

$$\times \Bigg[\left(3 - 6\frac{(2\mathcal{A}-1)}{4}[2nL+X]^2\right)e^{-2\mathcal{A}T}$$

$$- \left(2 - 4\frac{(4\mathcal{A}-1)}{4}[2nL+X]^2\right)e^{-4\mathcal{A}T}$$

$$- \left(1 - 2\frac{(1.2\mathcal{A}-1)}{4}[2nL+X]^2\right)e^{-1.2\mathcal{A}T}\Bigg]\Bigg\}H(T)$$

Similarly, for the case when a spike train is considered, all that is required is to replace all occurrences of T on the LHS of the expression for $\Phi_0(X, T)$ with $T - k\omega$ then the expression for $\Phi_0(X, T)$ is given by,

$$\Phi_0(X,T) = \frac{U_0}{\sqrt{\pi}U_{peak}}\sum_{k=0}^{m}\sum_{n=0}^{\infty}(-1)^n e^{-0.2A(T-k\omega)}\Bigg\{$$

$$\sin\left(\frac{2}{5}\pi\mathcal{A}(T-k\omega)\right)\sqrt{\pi}Erfc\left(\frac{[2(n+1)L-X]}{2\sqrt{T-k\omega}}\right)$$

$$+ \sin\left(\frac{2}{5}\pi\mathcal{A}(T-k\omega)\right)\Bigg[(0.2\mathcal{A}-1)[2(n+1)L-X]$$

$$\times \sqrt{T - k\omega}\exp\left(-\frac{[2(n+1)L - X]^2}{4(T - k\omega)}\right)$$

$$- (0.2\mathcal{A} - 1)\left(\frac{[2(n+1)L - X]^2)}{4}\right)\sqrt{T - k\omega}$$

$$\times 2\sqrt{\pi}Erfc\left(\frac{[2(n+1)L - X]}{2\sqrt{T - k\omega}}\right)\Big]$$

$$- \cos\left(\frac{2}{5}\pi\mathcal{A}(T - k\omega)\right)\left(\frac{[2(n+1)L - X]^2}{4}\right)$$

$$\times \sqrt{\pi}Erfc\left(\frac{[2(n+1)L - X]}{2\sqrt{T - k\omega}}\right)$$

$$- \cos\left(\frac{2}{5}\pi\mathcal{A}(T - k\omega)\right)(0.2\mathcal{A} - 1)$$

$$\times \left(\frac{[2(n+1)L - X]^3}{4}\right)$$

$$\times \sqrt{T - k\omega}\exp\left(-\frac{[2(n+1)L - X]^2}{4(T - k\omega)}\right)$$

$$+ \cos\left(\frac{2}{5}\pi\mathcal{A}(T - k\omega)\right)(0.2\mathcal{A} - 1)$$

$$\times \left(\frac{[2(n+1)L - X]^2}{4}\right)^2$$

$$\times 2\sqrt{\pi}Erfc\left(\frac{[2(n+1)L - X]}{2\sqrt{T - k\omega}}\right)$$

$$+ \sin\left(\frac{2}{5}\pi\mathcal{A}(T - k\omega)\right)\sqrt{\pi}Erfc\left(\frac{[2nL + X]}{2\sqrt{T - k\omega}}\right)$$

$$+ \sin\left(\frac{2}{5}\pi\mathcal{A}(T - k\omega)\right)\Big[(0.2\mathcal{A} - 1)$$

$$\times [2nL + X]\sqrt{T - k\omega}\exp\left(-\frac{[2nL + X]^2}{4(T - k\omega)}\right)$$

$$- (0.2\mathcal{A} - 1)\left(\frac{[2nL + X]^2}{4}\right)\sqrt{T - k\omega}$$

$$\times 2\sqrt{\pi}Erfc\left(\frac{[2nL + X]}{2\sqrt{T - k\omega}}\right)\Big]$$

$$- \cos\left(\frac{2}{5}\pi\mathcal{A}(T - k\omega)\right)\left(\frac{[2nL + X]^2}{4}\right)$$

$$\times \sqrt{\pi}Erfc\left(\frac{[2nL + X]}{2\sqrt{T - k\omega}}\right)$$

$$- \cos\left(\frac{2}{5}\pi\mathcal{A}(T - k\omega)\right)(0.2\mathcal{A} - 1)\left(\frac{[2nL + X]^3}{4}\right)$$

$$\times \sqrt{T - k\omega}\exp\left(-\frac{[2nL + X]^2}{4(T - k\omega)}\right)$$

$$+ \cos\left(\frac{2}{5}\pi\mathcal{A}(T - k\omega)\right)(0.2\mathcal{A} - 1)\left(\frac{[2nL + X]^2}{4}\right)^2$$

$$\times 2\sqrt{\pi}Erfc\left(\frac{[2nL + X]}{2\sqrt{T - k\omega}}\right)\Big\}$$

$$+ \frac{50U_0}{\sqrt{\pi}U_{peak}}\Big\{4[2(n+1)L - X]\sqrt{T - k\omega}$$

$$\times \exp\left(\frac{[2(n+1)L - X]^2}{4(T - k\omega)}\right)\Big[3\frac{(2\mathcal{A} - 1)}{4}e^{-2\mathcal{A}(T - k\omega)}$$

$$- 2\frac{(4\mathcal{A} - 1)}{4}e^{-4\mathcal{A}(T - k\omega)}$$

$$- \frac{(1.2\mathcal{A} - 1)}{4}e^{-1.2\mathcal{A}(T - k\omega)}\Big]$$

$$+ \sqrt{\pi}\,Erfc\left(\frac{[2(n+1)L - X]}{\sqrt{4(T - k\omega)}}\right)$$

$$\times \Big[\left(3 - 6\frac{(2\mathcal{A} - 1)}{4}[2(n+1)L - X]^2\right)e^{-2\mathcal{A}(T - k\omega)}$$

$$- \left(2 - 4\frac{(4\mathcal{A} - 1)}{4}[2(n+1)L - X]^2\right)e^{-4\mathcal{A}(T - k\omega)}$$

$$- \left(1 - 2\frac{(1.2\mathcal{A} - 1)}{4}[2(n+1)L - X]^2\right)$$

$$\times e^{-1.2\mathcal{A}(T - k\omega)}\Big]\Big\}H(T - k\omega)$$

$$+ \frac{50U_0}{\sqrt{\pi}U_{peak}}\Big\{4[2nL + X]\sqrt{T - k\omega}$$

$$\times \exp\left(\frac{[2nL + X]^2}{4(T - k\omega)}\right)\Big[3\frac{(2\mathcal{A} - 1)}{4}e^{-2\mathcal{A}(T - k\omega)}$$

$$- 2\frac{(4\mathcal{A} - 1)}{4}e^{-4\mathcal{A}(T - k\omega)}$$

$$- \frac{(1.2\mathcal{A} - 1)}{4}e^{-1.2\mathcal{A}(T - k\omega)}\Big]$$

$$+ \sqrt{\pi}Erfc\left(\frac{[2nL + X]}{\sqrt{4(T - k\omega)}}\right)\times$$

$$\Big[\left(3 - 6\frac{(2\mathcal{A} - 1)}{4}[2nL + X]^2\right)e^{-2\mathcal{A}(T - k\omega)}$$

$$- \left(2 - 4\frac{(4\mathcal{A} - 1)}{4}[2nL + X]^2\right)e^{-4\mathcal{A}(T - k\omega)}$$

$$- \left(1 - 2\frac{(1.2\mathcal{A} - 1)}{4}[2nL + X]^2\right)$$

$$\times e^{-1.2\mathcal{A}(T - k\omega)}\Big]\Big\}H(T - k\omega)$$

where $Erfc(z)$ is the complementary error function.

References

Aiello, G. L. & Bach-y Rita, P. (1997) Brain cell microenvironment effects on neuron excitability and basal metabolism. *NeuroReport* **8**, 1165–1168.

Altenberger, R., Lindsay, K., Ogden, J. & Rosenberg, J. (2001) The interaction between membrane kinetics and membrane geometry in the transmission of action potentials in non-uniform excitable fibres: a finite element approach. *Journal of Neuroscience Methods* **112**, 101–117.

Antic, S. D. (2003) Action potentials in basal and oblique dendrites of rat neocortical pyramidal neurons. *Journal of Physiology (London)* **550**, 35–50.

Ballou, E. W., Smith, W. B., Anelli, R. & Heckman,C. (2006) Measuring dendritic distribution of membrane proteins. *Journal of Neuroscience Methods* **156**, 257–266.

Bischofberger, J. & Jonas, P. (1997) Action potential propagation into the presynaptic dendrites of rat mitral cells. *Journal of Physiology (London)* **504**, 359–365.

Callaway, J. C. & Ross, W. N. (1995) Frequency dependent propagation of sodium action potentials in dendrites of hippocampal CA1 pyramidal neurons. *Journal of Neurophysiology* **74**, 1395–1403.

Cao, B. J. & Abbott, L. F. (1993) A new computational method for cable theory problems. *Biophysical Journal*, **64**, 303–313.

Casten, R. G., Cohen, H. & Lagerstrom, P. A. (1975) Perturbation analysis of an approximation to the Hodgkin-Huxley theory. *Quarterly of Applied Mathematics* **32**, 365–402.

Chen, W. R., Shen, G. Y., Shepherd, G. M., Hines, M. L. & Midtgaard, J. (2002) Multiple modes of action potentialinitiation and propagation in mitral cell primary dendrite. *Journal of Neurophysiology* **88**, 2755–2764.

Chiang, C. (1978) On the nerve impulse equation: the dynamic responses of nerve impulse. *Bulletin of Mathematical Biology* **40**, 247–255.

Chiu, S., Ritchie, J., Rogart, R. & Stagg, D. (1979) A quantitative description of membrane currents in rabbit myelinated nerve. *Journal of Physiology (London)* **292**, 149–166.

Colbert, C. M., Magee, J. C., Hoffman, D. A. & Johnston, D. (1997) Slow recovery from inactivation of Na^+ channels underlies the activity-dependent attenuation of dendritic action potentials in hippocampal ca1 pyramidal neurons. *Journal of Neuroscience* **17**, 6512–6521.

Dimitrova, N. A. & Dimitrov, G. V. (1991) Difference in excitability along geometrically inhomogeneous structures and occurrence of "hotspots". *Biological Cybernetics* **66**, 185–189.

Dodge, F. & Frankenhaeuser, B. (1959) Sodium currents in the myelinated nerve fibre of *xenopus laevis* investigated with the voltage clamp technique. *Journal of Physiology (London)* **148**, 188-200.

Doiron, B., Longtin, A., Turner, R. W. & Maler, L. (2001) Model of gamma frequency burst discharge generated by conditional backpropagation. *Journal of Neurophysiology* **86**, 1523–1545.

Ehrenstein, G. & Lecar, H. (1972) The mechanism of signal transmission in nerve axons. *Annual Review of Biophysics and Bioengineering* **1**, 347–366.

Evans, J. & Shenk, N. (1970) Solutions to axon equations. *Biophysical Journal* **10**, 1090–1101.

FitzHugh, R. (1960) Thresholds and plateaus in the Hodgkin-Huxley nerve equations. *The Journal of General Physiology* **43**, 867–896.

FitzHugh, R. (1973) Dimensional analysis of nerve models. *Journal of Theoretical Biology* **40**, 517–541.

Fleidervish, I. A., Friedman, A. & Gutnick, M. J. (1996) Slow inactivation of Na^+ current and slow cumulative spike adaptation in mouse and guinea-pig neocortical neurones inslices. *Journal of Physiology(London)* **493**, 83–97.

Frankenhaeuser, B. & Huxley, A. (1964) The action potential in the myelinated nerve fibre of *xenopus laevis* as computed on the basis of voltage clamp data. *Journal of Physiology (London)* **171**, 302-315.

Frick, A., Zieglgansberger, W. & Dodt, H.-U. (2001) Glutamate receptors form hotspots on apical dendrites of neocortical pyramidal neurons. *Journal of Neurophysiology* **86**, 1412–1421.

Golding, N. L., Kath, W. L. & Spruston, N. (2001) Dichotomy of action-potential backpropagation in ca1 pyramidal neuron dendrites. *Journal of Neurophysiology* **86**, 2998–3010.

Hille, B. (2001) *Ionic Channels of Excitable Membranes*, 3rd ed., Sinauer, Sunderland, MA.

Hodgkin, A. L. & Huxley, A. F. (1952) A quantitative description of membrane current and its application to conduction and excitation in nerve. *Journal of Physiology (London)* **117**, 500–544.

Hodgkin, A. L. (1975), 'The optimum density of sodium channels in an unmyelinated nerve. *Philosophical Transactions of the Royal Society of London.* **B 270**, 297–300.

Hoffman, D. A., Magee, J. C., Colbert, C. M. & Johnston, D. (1997) K^+ channel regulation of signal propagation in dendrites of hippocampal pyramidal neurons. *Nature* **387**, 869–875.

Holden, A. (1980) Autorhythmicity and entrainment in excitable membranes. *Biological Cybernetics* **38**, 1–8.

Holden, A. (1981) Membrane current fluctuations and neuronal information processing. In G. Szekely (Ed.) *Neural Communication and Control.* Pergamon Press, Oxford.

Holden, A. V. & Winlow, W. (1983) Neuronal activity as the behavior of a differential system. *IEEE Transactions on Systems, Man, and Cybernetics* **13**, 711–719.

Horikawa, Y. (1998) Bifurcations in the decremental propagation of a spike train in the Hodgkin-Huxley model of low excitability. *Biological Cybernetics* **79**, 251–261.

Huguenard, J. R., Hamill, O. P. & Prince, D. A. (1989) Sodium channels in dendrites of rat cortical pyramidal neurons. *Proceedings of the National Academy of Sciences (USA)* **86**, 2473–2477.

Iannella, N. & Tanaka, S. (2006) Analytical solutions for nonlinear cable equations with calcium dynamics. I. Derivations. *Journal of Integrative Neuroscience* **5**, 249–272.

Iannella, N. Launcy,T. Abbott, D. & Tanaka, S. (2014) A nonlinear cable framework for bidirectional synaptic plasticity. *PLoS One* **9**, 102601.

Jack, J.J.B. , Noble, D. &Tsein, R. (1983) *Electric Current Flow in Excitable Cells*. Clarendon Press, Oxford.

Jaffe, D. B., Johnston, D., Lasser-Ross, N., Lisman, J. E., Miyakawa, H. & Ross, W. N. (1992) The spread of Na$^+$ spikes determines the pattern of dendritic Ca^{2+} entry into hippocampal neurons. *Nature* **357**, 244–246.

Johnston, D., Magee, J. C., Colbert, C. M. & Christie, B. R. (1996), Active properties of neuronal dendrites. *Annual Review of Neuroscience* **19**, 165–186.

Jung, H.-Y., Mickus, T. & Spruston, N. (1997) Prolonged sodium channel inactivation contributes to dendritic action potential attenuation in hippocampal pyramidal neurons. *Journal of Neuroscience* **17**, 6639–6646.

Kepler, T. B., Abbott, L. & Marder, E. (1992) Reduction of conductance-based neuron models. *Biological Cybernetics* **66**, 381–387.

Krinskii, V. & Kokoz, Y. M. (1973) Analysis of equations of excitable membranes-I. Reduction of the Hodgkin-Huxley equations to a second order system. *Biophysics* **18**, 533–539.

Lai, H. C. & Jan, L. Y. (2006) The distribution and targeting of neuronal voltage-gated ion channels. *Nature Reviews Neuroscience* **7**, 548–562.

Lemon, N. & Turner, R. (2000) Conditional spike backpropagation generates burst discharge in a sensory neuron. *Journal of Neurophysiology* **84**, 1519–1530.

Lüscher, H.-R. & Larkum, M. E. (1998) Modeling action potential initiation and back-propagation in dendrites of cultured rat motoneurons. *Journal of Neurophysiology* **80**, 715–729.

Magee, J. C. (1998) Dendritic hyperpolarization-activated currents modify the integrative properties of hippocampal CA1 pyramidal neurons. *Journal of Neuroscience* **18**, 7613–7624.

Magee, J. C. & Johnston, D. (1995) Characterization of single voltage-gated Na$^+$ and Ca^{2+} channels in apical dendrites of rat CA1 pyramidal neurons. *Journal of Physiology (London)* **487**, 67–90.

Mainen, Z. F., Joerges, J., Huguenard, J. R. & Sejnowski,T. J. (1995) A model of spike initiation in neocorticalpyramidal cells. *Neuron* **15**, 1427–1439.

Markram, H., Helm, P. J. & Sakmann, B. (1995) Dendritic calcium transients evoked by single back-propagating actionpotentials in rat neocortical pyramidal neurons. *Journal of Physiology (London)* **485**, 1–20.

Maršálek, P. & Santamarıa, F. (1998) Investigating spike backpropagation induced Ca^{2+} influx in models of hippocampal and cortical pyramidal neurons. *Biosystems* **48**, 147–156.

Mascagni, M. (1989) An initial-boundary value problem of physiological significance for equations of nerve conduction. *Communication in Pure and Applied Mathematics* **42**, 213–227.

McKeown, L., Swanton, L., Robinson, P. & Jones, O. T. (2008) Surface expression and distribution of voltage-gated potassium channels in neurons. *Molecular Membrane Biology* **25**, 332–343.

Mel, B. W. (1993) Synaptic integration in an excitable dendritic tree. *Journal of Neurophysiology* **70**, 1086–1101.

Mickus, T., Jung, H.-Y. & Spruston, N. (1999) Properties of slow, cumulative sodium channel inactivation in rat hippocampal ca1 pyramidal neurons. *Biophysical Journal* **76**, 846–860.

Migliore, M. (1996) Modeling the attenuation and failure of action potentials in the dendrites of hippocampal neurons. *Biophysical Journal* **71**, 2394–2403.

Migliore, M. (2003) On the integration of subthreshold inputs from perforant path and schaffer collaterals in hippocampal CA1 pyramidal neurons. *Journal of Computational Neuroscience* **14**, 185–192.

Migliore, M., Hoffman, D. A., Magee, J. C. & Johnston,D. (1999) Role of an A-type K$^+$ conductance in the back-propagation of action potentials in the dendrites of hippocampal pyramidal neurons. *Journal of Computational Neuroscience* **7**, 5–15.

Migliore, M. & Shepherd, G. M. (2002) Emerging rules forthe distributions of active dendritic conductances'. *Nature Reviews Neuroscience* **3**, 362–370.

Miller, R. F. & Dacheux, R. (1976) Dendritic and somatic spikes in mudpuppy amacrine cells: identification and TTX sensitivity. *Brain Research* **104**, 157–162.

Misonou, H. & Trimmer, J. S. (2004) Determinants of voltage-gated potassium channel surface expression and localization in mammalian neurons. *Critical Reviews in Biochemistry and Molecular Biology* **39**, 125–145.

Moore, J. W. & Adelman Jr, W. J. (1961) Electronic measurement of the intracellular concentration and net flux of sodium in the squid axon. *Journal of General Physiology* **45**, 77–92.

Mozrzymas, J. W. & Bartoszkiewicz, M. (1993) The discrete nature of biological membrane conductance channelinteration through electrolyte layers and the cable equation. *Journal of Theoretical Biology* **162**, 371–380.

Penney, M. & Britton, N. (2002) Modelling natural burst firing in nigral dopamine neurons. *Journal of Theoretical Biology* **219**, 207–223.

Pickard, W. F. (1974) Electrotonus on a nonlinear dendrite. *Mathematical Biosciences* **20**, 75–84.

Poirazi, P., Brannon, T. & Mel, B. W. (2003) Pyramidal neuron as two-layer neural network. *Neuron* **37**, 989–999

Poznanski, R. R. (2001) Conduction velocity of dendritic potentials in a cultured hippocampal neuron model. *Neuroscience Research Communications* **28**, 141–150.

Poznanski, R. R. (2004) Analytical solutions of the Frankenhaeuser-Huxley equations. I. Minimal model for backpropagation of action potentials in sparsely excitable dendrites. *Journal of Integrative Neuroscience* **3**, 267–299.

Poznanski, R. R. & Bell, J. (2000*a*) A dendritic cable model for the amplification of synaptic potentials by an ensemble average of persistent sodium channels. *Mathematical Biosciences* **166**, 101–121.

Poznanski, R. R. & Bell, J. (2000*b*) Theoretical analysis of the amplification of synaptic potentials by small clusters of persistent sodium channels in dendrites. *Mathematical Biosciences* **166**, 123–147.

Poznanski, R. R., Cacha, L. A., Al-Wesabi, Y. M. S., Ali, J., Bahadoran, M., Yupapin, P. P., and Yunus, J. (2017a) Solitonic conduction of electrotonic signals in neuronal branchlets with polarized microstructure. *Scientific Reports* **7**, 2746.

Poznanski, R. R., Cacha, L. A., Ali, J., Rizvi, Z. H., Yupapin, P., Salleh, S. H., and Bandyopadhyay, A. (2017b). Induced mitochondrial membrane potential for modelling solitonic conduction of electrotonic signals. *PLoS One* **12**, e0183677.

Qian, N. & Sejnowski, T. (1989) An electro-diffusion model for computing membrane potentials and ionic concentrations in branching dendrites, spines and axons. *Biological Cybernetics* **62**, 1–15.

Rall, W. (1959) Branching dendritic trees and motoneuron membrane resistivity. *Experimental Neurology* **1**, 491–527.

Rapp, M., Yarom, Y. & Segev, I. (1996) Modeling back propagating action potential in weakly excitable dendrites of neocortical pyramidal cells. *Proceedings of the National Academy of Sciences (USA)* **93**, 11985–11990.

Regehr, W., Kehoe, J., Ascher, P. & Armstrong, C. (1993) Synaptically triggered action potentials in dendrites. *Neuron* **11**, 145–151.

Reyes, A. (2001) Influence of dendritic conductances on the input-output properties of neurons. *Annual Review of Neuroscience* **24**, 653–675.

Rinzel, J. (1985) Excitation dynamics: insights from simplified membrane models. *Federal Proceedings* **44**, 2944–2946.

Rissman, P. (1977) The leading edge approximation to the nerve axon problem. *Bulletin of Mathematical Biology* **39**, 43–58.

Sabah, N. & Leibovic, K. (1969) Subthreshold oscillatory responses of the Hodgkin-Huxley cable model for the squid giant axon. *Biophysical Journal* **9**, 1206–1222.

Sabah, N. & Leibovic, K. (1972) The effect of membrane parameters on the properties of the nerve impulse. *Biophysical Journal* **12**, 1132–1144.

Schaefer, A. T., Larkum, M. E., Sakmann, B. & Roth, (2003) Coincidence detection in pyramidal neurons is tuned by their dendritic branching pattern. *Journal of Neurophysiology* **89**, 3143–3154.

Scott, A. (2002) *Neuroscience: A Mathematical Primer*, Springer-Verlag, Berlin.

Sheng, M., Tsaur, M.-L., Jan, Y. N. & Jan, L. Y. (1992) Subcellular segregation of two A-type K^+ channel proteins in rat central neurons. *Neuron* **9**, 271–284.

Sigworth, F. J. & Neher, E. (1980) Single Na^+ channel currents observed in cultured rat muscle cells. *Nature* **287**, 447–449.

Stuart, G. & Häusser, M. (1994) Initiation and spread of sodium action potentials in cerebellar Purkinje cells. *Neuron* **13**, 703–712.

Stuart, G. & Spruston, N. (1995) Invited commentary: Probing dendritic function with patch pipettes. *Current Opinion in Neurobiology* **5**, 389–394.

Stuart, G. & Spruston, N. (1998) Determinants of voltage attenuation in neocortical pyramidal neuron dendrites. *Journal of Neuroscience* **18**, 3501–3510.

Stuart, G., Spruston, N., Sakmann, B. & Häusser, M. (1997) Action potential initiation and backpropagation in neuronsof the mammalian CNS. *Trends in Neurosciences* **20**, 125–131.

Stühmer, W., Methfessel, C., Sakmann, B., Noda, M.& Numa, S. (1987) Patch clamp characterization of sodium channels expressed from rat brain cDNA. *European Biophysics Journal* **14**, 131–138.

Taylor,G. Coles,J. & Eilbeck,J. (1995) Mathematical modelling of weekly nonlinear pulses in a retinal neuron. Chaos, Solitons & Fractals **5,** 407-413.

Trimmer, J. S. & Rhodes, K. J. (2004) Localization of voltage-gated ion channels in mammalian brain. *Annual Review of Physiology* **66**, 477–519.

Troy, W. C. (1977) Large amplitude periodic solutions of a system of equations derived from the Hodgkin-Huxley equations. *Archive for Rational Mechanics and Analysis* **65**, 227–247.

Tuckwell, H. C. (1988) *Introduction to Theoretical Neurobiology, vol 1, Linear Cable Theory and Dendritic Structure*. Cambridge University Press, New York.

Turner, R., Maler, L., Deerinck, T., Levinson, S. & Ellisman, M. (1994) TTX-sensitive dendritic sodium channels underlie oscillatory discharge in a vertebrate sensory neuron. *Journal of Neuroscience* **14**, 6453–6471.

Van Ooyen, A., Duijnhouwer, J., Remme, M. W. & van Pelt, J. (2002). The effect of dendritic topology on firing patterns in model neurons. *Network: Computation in Neural Systems* **13**, 311-325.

Vandenberg, C. & Bezanilla, F. (1991) Single-channel, macroscopic, and gating currents from sodium channels in the squid giant axon. *Biophysical Journal* **60**, 1499–1510.

Williams, S. R. & Stuart, G. J. (2000) Backpropagation of physiological spike trains in neocortical pyramidal neurons: implications for temporal coding in dendrites. *Journal of Neuroscience* **20**, 8238–8246.

Wilson, H. R. (1999) Simplified dynamics of human and mammalian neocortical neurons. *Journal of Theoretical Biology* **200**, 375–388.

Xiong, W. and Chen, W. R. (2002) Dynamic gating of spike propagation in the mitral cell lateral dendrites. *Neuron* **34**, 115–126.

Yamada, Y., Koizumi, A., Iwasaki, E., Watanabe, S.-I., and Kaneko, A. (2002) Propagation of action potentials from the soma to individual dendrite of cultured rat amacrine cells is regulated by local GABA input. *Journal of Neurophysiology* **87**, 2858-2866.